YASAR UNIVERSITY
GRADUATE SCHOOL OF NATURAL AND APPLIED SCIENCES

MASTER THESIS

DESIGN AND IMPLEMENTATION OF AN ELECTROMAGNETIC TARGET CLASSIFICATION METHOD USING HIGH FREQUENCY RESOLUTION TECHNIQUES AND TIME-FREQUENCY REPRESENTATIONS

Salih POYRAZ

Thesis Advisor: Assoc. Prof. Dr. Mustafa SEÇMEN

Department of Electrical & Electronics Engineering

Presentation Date: 21.05.2015

Bornova-İZMİR
2015

1

I certify that I have read this thesis and that in my opinion it is fully adequate, in scope and in quality, as a dissertation for the degree of master of science.

Assoc. Prof. Dr. Mustafa SEÇMEN (Supervisor)

I certify that I have read this thesis and that in my opinion it is fully adequate, in scope and in quality, as a dissertation for the degree of master of science.

Assist. Prof. Dr. Muammer ÇATAK

I certify that I have read this thesis and that in my opinion it is fully adequate, in scope and in quality, as a dissertation for the degree of master of science.

Assist. Prof. Dr. Nalan ÖZKURT

Prof. Dr. Behzat GÜRKAN
Director of the Graduate School

ABSTRACT

DESIGN AND IMPLEMENTATION OF AN ELECTROMAGNETIC TARGET CLASSIFICATION METHOD USING HIGH FREQUENCY RESOLUTION TECHNIQUES AND TIME-FREQUENCY REPRESENTATIONS

Poyraz, Salih

MSc in Electrical and Electronics Engineering

Supervisor: Assoc. Prof. Dr. Mustafa SEÇMEN

May 2015, 64 pages

In this thesis, it is aimed to develop a fast and sufficient target classification method, which is independent from aspect angle and polarization. By processing the scattered radar signals, a method having low decision time and high accuracy rates even at high noise levels, are expected. In thesis, it is assumed that a certain number of targets to be classified are in resonance scattering region. Besides, it is assumed that predetermined and moderate number of reference signals corresponding to different angle/polarization cases is available for each target. In the first part of the suggested method, by using high resolution techniques such as ESPRIT, Min-Norm, MUSIC, some feature vectors are obtained in real frequency domain. However, the proposed method requires the vectors as the number of reference signals for each target and here the problem is that a serious increament of decision time. For this reason, in the second stage of suggested method, it is aimed to decrease the number of feature vectors to one by applying dimension reduction technique or high resolution techniques for multiple signals to these vectors. In this way, decision speed can be faster and system memory may be used more sufficiently. In the test stage, the scattered signal concerning to any angle/polarization case of a target is processed with the same high resolution technique and a test vector is formed. Finally, classification beetween test vector and feature vectors is done by the help of highest correlation coefficients. Thus, a radar target classification method independent from angle and polarization as possible under high noise situations is constituted.

In the suggested project, after some comparisons and trials signal processing methods are chosen for best effort as ESPRIT and principal component analysis (PCA).

In second stage of study, for the given method, essential optimum late-time intervals of the scattered signals are determined by using time-frequency representations. The time instants, independent from targets positions, are applied which are belong to maximum and mean power values in time-frequency distributions. Then, the feature vectors are formed for each target by using the given time-frequency distributions over these selected late-time regions at several different reference aspects and they are eventually used for the classification in test stage. In this thesis, two different strategies are created as "target-specific" and "signal-specific" late-time intervals. The lossless dielectric spheres are used for the simulations. The performances of designed strategies as well as other similar methods in the literature are compared for various well-known time-frequency representations.

Keywords: Radar target classification, resonance scattering region, high resolution techniques, dimension reduction

ÖZET

YÜKSEK ÇÖZÜNÜRLÜK VE ZAMAN-FREKANS DAĞILIM TEKNİKLERİNİ KULLANAN BİR ELEKTROMANYETİK HEDEF SINIFLANDIRMA YÖNTEMİNİN TASARIMI VE GERÇEKLEŞTİRİLMESİ

Salih POYRAZ

Yüksek Lisans Elektrik-Elektronik Mühendisliği Bölümü

Tez Danışmanı: Doç. Dr. Mustafa SEÇMEN

Mayıs 2015, 64 sayfa

Bu çalışmada temel amaç hedeflerden saçılan geniş bantlı radar sinyallerinin işlenmesiyle, hızlı ve yeteri kadar açı ve polarizasyondan bağımsız bir hedef sınıflandırma yönteminin geliştirilmesidir. Aynı zamanda mümkün olduğunca geliştirilen yöntemin düşük karar verme süresine ve yüksek gürültü seviyelerinde bile başarılı doğruluk oranlarına sahip olması hedeflenmektedir. Önerilen yöntemlerde sınıflandırılması planlanan belli sayıda hedefin rezonans bölgesinde olduğu öngörülmektedir. Çalışmada her hedef için önceden seçilmiş ve makul sayıda farklı referans açı/polarizasyon durumuna ait zaman saçılım sinyallerinin elde edildiği varsayılmaktadır. Yöntemin öznitelik çıkarma kısmında herbir hedefin öznitelik vektörlerinin çıkarılması için ESPRIT, MUSIC ya da Min-Norm gibi yüksek çözünürlük teknikleri kullanılmıştır. Bu aşamada her referans sinyali için bir vektör elde edilir. Bu durum test aşamasında karar verme süresinin ciddi oranda artışına neden olacaktır. Bu yüzden öznitelik çıkarımının ikinci aşamasında bu vektörlere boyut azaltma tekniği ya da çoklu sinyaller için yüksek çözünürlük tekniği uygulanarak herbir hedefe ait öznitelik vektör sayısının bire indirilmesi amaçlanmaktadır. Bunun gerçekleştirilmesi yöntem için depolanan verinin azalmasına ve karar verme süresinin düşmesine yardımcı olur. Test aşamasında ise, bir test hedefinin herhangi bir açı/polarizasyon durumuna ait saçılım sinyali, aynı yüksek çözünürlük tekniği ile işlenecek ve bir test vektörü oluşturulmuştur. Sınıflandırma işi test vektörü ile öznitelik vektörleri arasındaki en yüksek ilinti katsayısına göre gerçekleştrilir. Bu yüksek gürültü şartlarında bile mümkün olduğunca açı ve polarizasyondan bağımsız hızlı bir radar hedef sınıflandırma yöntemi gerçekleştirmeyi sağlamaktadır. Önerilen çalışmada vektörler esas olarak

ESPRIT ve temel bileşenler analizi (TBA) gibi sinyal işleme teknikleri yardımıyla oluşturulmuştur ve literatürdeki benzer çalışmalar daha iyi performans elde edilmiştir.

Çalışmanın ikinci aşaması ise hedeflerin boyutlarının dalgaboyuna yakın olduğu rezonans saçılım bölgesindeki hedeflerin sınıflandırılması amacıyla literatürde ve bu çalışmada önerilen Wigner dağılımı tabanlı radar hedef sınıflandırma yöntemlerin performanslarının kıyaslanmasını içermektedir. Önerilen yöntemlerde hedeflerden saçılan sinyallerin teorisinde kritik olan optimum geç-zaman aralıkları, sinyallerin Wigner enerji haritaları kullanılarak tespit edilmiştir. Daha sonra, seçilen bu geç-zaman aralıklarında, her hedef için farklı referans açılarına ait sinyallerin Wigner dağılımları ve boyut azaltma tekniği olarak temel bileşen analizi kullanılarak hedeflerin öznitelik vektörleri elde edilmiştir. Bu vektörler test aşamasında sınıflandırma amacıyla kullanılmıştır. Önerilen yöntemler literatürdeki benzer yöntemlere göre hedeflerin bulunduğu pozisyondan bağımsız olma ve kutupların sayı ve değerlerinin yüksek hassasiyet ile bulunmasına ihtiyaç olmama gibi önemli sayılabilecek özelliklere sahiptirler. Çalışmada geometrik olarak basit fakat saçılım mekanizması olarak karmaşık hedefler olan kayıpsız yalıtkan küreler ile testler yapılmış ve özellikle hedeflere özgü optimum geç-zaman aralıklarına sahip yöntemin daha başarılı olduğu bulunmuştur.

Anahtar sözcükler: radar hedef sınıflandırma; elektromanyetik rezonans saçılım bölgesi; Yüksek çözünürlük teknikleri, Boyut azaltma yöntemleri

ACKNOWLEDGEMENTS

TEXT OF OATH

I declare and honestly confirm that my study, titled "Design and implementation of an electromagnetic target classification method using High Frequency Resolution techniques and Time-Frequency Representations" and presented as a Master Thesis, has been written without applying to any assistance inconsistent with scientific ethics and traditions, that all sources from which I have benefited are listed in the bibliography, and that I have benefited from these sources by means of making references.

TABLE OF CONTENTS

Page

INDEX OF FIGURES

INDEX OF TABLES

1   INTRODUCTION

1.1   Subject of the Thesis

Radar target recognition and classification is an important topic because it has wide usage areas such as military applications, medical applications, security systems. In this kind of applications; methods generally use the scattered signals to recognize and clasify the features of targets. These feature vectors can be related with size, shape or type of material directly or indirectly. As the result of studies in the recent years, many applications try to define some other informations (location, speed, etc.) beside defining the presence of the target. Type of the target should be defined with high accuracy in many applications. In this sense, electromagnetic target classificiation is an important and complex problem. The main purpose in radar target classification methods is to clasify the target by the help of comparison between target features and test target features. These features are extracted from scattered signals coming from the target. But feature vectors are highly dependent on the aspect angle, polarization and freqeuncy so suggested method should be independent from these parameters as possible. However, noise also can reduce the accuracy rates in the classification stage. Other important parameter is runtime for the methods such that decision time should be fast enough in the classification stage for real time applications.

According to the wavelength of incoming signal, an electromagnetic target has 3 different scattering region (Rayleigh, resonance and optical). The methods used in modeling of target detection and classification problems of electromagnetic scattering signals, show the fundamental differences according to different frequency regions. In case of where the target size is close to wavelength, if the scattered signals are obtained with wide-band radar, the measured signals can be used for target classification. The late-time intervals based on singularity expansion method consist of the summation of the detected numerous oscillating damped sinusoidals in complex poles. The electromagnetic signals that relatively less sensitive to the incidence angle are examined in the framework of several linear system models and processed by signal processing techniques and the resulting target specific attributes are available to use in the target classifier design. To benefit from these attributes dependencies on angle and polarization and sensitivity on noise should be low as possible.

1.2   Aims and Problem Definition

The aim of this project is to develop a resonance region target recognition and classification method which has low dependency on angle and polarization, less sensitive to noise level, with high accuracy rates and low decision time. The method developed in the thesis are based on the use of high resolution techniques and dimension reduction technique. MUSIC, Min-Norm and ESPRIT are well-known methods and frequently used in many applications (Dogan and Mendel, 1993; Georgiou, 2000; Burrows, 2004; Lobos, 2006; Gokalp, 2010). However, few studies are observed in literature for target classification problems in resonance region except some studies (Secmen, 2008; Secmen and Turhan-Sayan, 2009; Vasalos, 2011a; Vasalos, 2011b). Although, especially the study of (Secmen, 2008) has shown positive signs for the use of classification of high resolution techniques, mentioned methods only used the MUSIC algorithm and relatively long decision time is observed. To overcome this problem, a radar target classification method is aimed to develop that give higher accuracy rates and shorter decision time in the thesis. For this purpose, a comparative study is made that include the comparative results of other high resolution techniques. During the studies, ESPRIT spectrum vector used as a new concept in literature for target recognition/classification and aimed to contribute to the literature.

Also time frequency representations are examined with two different explained methods as "signal specific" and "target specific" methods. This study is compared with the other studies by using the same parameters to get fair comparison. In proposed method, it is aimed to have better accuracy rates from the study of (Turhan Sayan, 2005). During the study some signal processing methods are tried such as STFT, Page, Wigner Ville, SPWV, PPG and Wigner method is found as the best method which gives higher accuracy rates and results.

1.3   Context of the Thesis

A detailed literature search will be given that including the studies are done recently. The details of the materials and methods used in the thesis will be explained. For example high resolution techniques such as MUSIC, Min-Norm and ESPRIT, dimension reduction techniques PCA, Average Value Method and Common Prediction Matrix and time frequency representations such as PAGE, STFT (short

time Fourier transform and Wigner Ville methods. Also materials and methods will be mentioned while obtaining scattered signals and steps and flowchart will be presented for radar target classification. Applications and result are also demonstrated with graphs and tables for time frequency representations and high frequency techniques with details and also necessary formulations, analytical/simulation scattering datas and measurement results will be also shown. These studies based on TFR's and high resolution techniques are compared with the other similar studies from the literature. All results and graphical datas are presented and the work planned for the future will be discussed briefly.

1.4   Structure of the Thesis

The method of this thesis is based on the radar target classification in the resonance region. As well as literature review of target classification and recognition worldwide.

There are not many studies on radar target classification in resonance region. In the thesis, related studies from literature are examined and same parameters are used for fairy comparison such as dimension of planes or dielectric spheres.

In Chapter 2, singularity expansion method (SEM) and literature examination have been presented with details.

In Chapter 3, the proposed radar target recognition with high resolution techniques were shown and MUSIC, Min-Norm, ESPRIT methods derscribes as high reolution techniques and PCA (Principal Component Analysis), Average Value Method and Common Prediction Matrix were shown as dimension reduction methods. Then in Chapter 4, application and results are demonstrated with figures, tables and simulations for applications of the proposed method.

Chapter 5 presented radar target recognition with time frequency representations. PAGE, STFT and Wigner-Ville methods were examined detaily. Especially proposed method focused on the Wigner-Ville method because of giving best performance. Then in Chapter 6, application and results are demonstrated with graphs, tables and simulations for these proposed method.

Chapter 7 includes the conclusion part and the future work for the proposed methods of "the proposed radar target recognition with high resolution techniques" and "the proposed radar target recognition with time frequency representations".

2   RESONANCE REGION TARGET RECOGNITION METHOD

An electromagnetic target has three different scattering regions when target size (d) is compared to operating wavelength (Rayleigh, resonance and optical). If the operating wavelength is much smaller than targets size (d>>λ), means that the scattering region is optical region, where radar systems generally operate at this region. If the target's size is defined as $0.1\lambda < d < 10\lambda$, the target is in resonance region, where creeping waves are very effective (Barton, 2005). Electromagnetic target recognition is important issue that includes security systems, biomedical applications and military applications such as land-mine detection. In the thesis, it is mainly aimed to develop a target classification method suitable for this resonance scattering region as in the mentioned applications, where targets dimensions are close to the wavelength of the incident electromagnetic signal of the application. In this region, scattering theory can be modeled with SEM (Singularity Expansion Method (Baum C. E., 1991)

2.1   Singularity Expansion Method

In target classification problems, a target can be modeled with a linear-time invariant system as shown in the Figure 2.1. where the dimension of target close to wavelength in scattering resonance region. Investigation of this model in resonance region was firstly made with singularity expansion method which is offered by C.E. Baum.
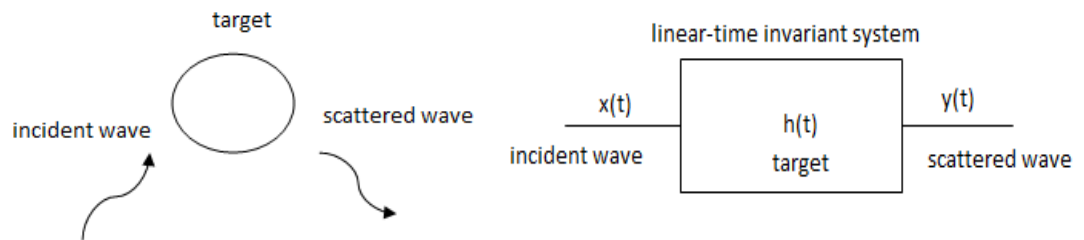
Figure 2.1 (a) Scattered electromagnetic signal (b) Linear and time invariant system model

According to singularıty expansion method, for a target in scattering resonance region, system function is shown below which is dependent on angle and polarization;

$$H(s,\Omega) = A(s,\Omega) + \sum_{n=1}^{\infty} \frac{R_n(s,\Omega)}{(s-s_n)(s-s_n^*)} \tag{2.1}$$

Here, Ω shows dependency on angle and polarization, $A(s, \Omega)$ shows an entire function which has no pole, $s_n = -\alpha_n \pm j\, 2\pi f_n$ describes system poles and $R_n(s, \Omega)$ points the residue of nth pole. The equation given in the Laplace domain, is specified in the time domain as shown below

$$h(t,\Omega) = a(t,\Omega) + \sum_{n} b_n(\Omega)\exp(-\alpha_n t)\cos(2\pi f_n t + \delta_n) \tag{2.2}$$

According to equation, the late-time intervals of the signals are the superposition of damped sinusoidals resonating at target's complex pole frequencies, Also those pole frequencies are called complex resonance frequencies. The most important property of these poles is that they are independent from polarization and aspect angle, and only related to shape of target, dimensions and material properties. This property provides characterization and classification of targets and system poles. In other words, if the system poles of target are known completely, target classification can be done correctly.

In equation, *a(t, Ω)* is a function of the force-response and only stays during the time interval (called as early time interval) of passing through of the incident wave over target. It means that $a(t, \Omega)$ function is a time-limited function. After early time interval ended only infinite summation part remains in the late time interval. In this part sine terms which are damping relatively rapid, fall to quite small noise level. On the remain part, sine terms of poles are obtained which damps slowly. These dominant terms and dominant poles related with sine terms are quiet important for target classification problems. Generally amplitudes of sine terms $b_n(\Omega)$, depends on angle and polarization so a dominant pole in case of certain angle/polarization situation may not behave as dominant because of small amplitude.

There are several methods to obtain some knowledge for transient scattered electromagnetic field in the late time period. The simplest way to calculate the transient response is to characterize the target by its impulse response first, and then to convolve this response with the incident waveform. In other words, all special

properties of a particular target can be understood from the study of its impulse response. A common method to compute the impulse response has been based upon Fourier Transform (FT) technique, e.g., (Moffatt, 1969). The problem with that approach is that slow convergence of the Fourier spectrum usually requires the inclusion of a large number of frequencies in numerical computation of impulse responses. The singularity expansion method (SEM) (Baum, 1978) expresses the transient response of a target in terms of its spectral-domain singularities, which normally exhibit a decaying behavior in the time domain. (C.I. Chuang, D. P. Nyquist, K.M. Chen, and B. C. Drachman, 1985), (Baum, 1978). Therefore SEM series usually converge faster, especially in the late-time period, and consequently require relatively few terms.

2.2   Summary of Literature

In this part of the study, publications which use the high resolution and dimension reduction technique that are related with radar target classfication and recognition are examined. While examining publications, this study focussed on resonance scattering region (where the dimension of the target close to wavelength). Optical region methods (where the dimension of the target bigger than wavelength) are ignored for this study, which should have to use many reference signals. The current publications in the literature can be summarized as follows:

In the study of Lee and his collegues (Lee, 2008; Huang and Lee, 2010a; Huang and Lee, 2010b), Principal Component Analysis and Independent Component Analysis are implemented succesfully and also results are given for noisy signals too. However, the size of the targets used in this study were selected quite different from each other (three target with size of L, 2L, 3L). Mentioned studies are explained for special occasions as where reference signals number equal to test signals number. On the other hand, when using independent components in radar target classification problems, created covariance matrix should be examined for deciding eigenvalue numbers. More importantly, number of reference signals becomes equal to the number of test signals in quite exceptional circumstances for these types of problems. Because the purpose is to decide with a small number of reference signals as possible about test signals as many as possible. In this sense, the above-mentioned shortcomings have been observed in these studies and the results should be examined again for the targets which dimensions are close to each other.

7

Lui and his colleagues, used quite known E-pulse method as a biomedical application to detect hip prosthesis under the skin and also successful results achieved for noisy signals (Lui, 2009; Lui, 2010; Lui and Shuley, 2010). But these studies also could not produce a solution to the main problem of E-pulse method and also any performance test or the results table for noisy signals is not included. To mention briefly the problems of E-pulse method, target poles are used while generating discriminative / recognizer pulses. However, the generated pulses, and thus target recognition performance is highly dependent on the number and value of the target poles (especially the pole with highest correlation coefficient) (Lui and Shuley, 2008). In the processing of finding target poles and numbers "generalized-pencil-of-matrix" (GPOF) or "Matrix pencil" the matrix is performed and magnitudes of the eigenvalues are examined (Sarkar and Pereira, 1995). But especially this method can give inconsistent results for noisy signals because of being very close to each other for eigenvalues. Moreover, in case of failure to identify target pole (due to low amplitude), even for a noiseless signal, generated pulses can rather vary. The studies mentioned previously do not include a solution for these problems.

Zhang and his colleagues created a genetic algorithm and found the target poles with certain accuracy rate. This method were tested for a security system application (hidden weapons) (Zhang, 2007; Zhang, 2011). In these tests, although pole values of concealed weapons were obtained with sufficient accuracy, it was not mentioned that poles were used for target classification/recognition purpose. Also optimization tools such as genetic algorithm may take a long time so undesirably this event may cause an significant increase on the decision time. This problem is mentioned in these studies but a solution about duration and improvement for target poles extraction time is not discussed.

Harmer and his colleagues, performed some studies to distinguish non-hazardous substances and ammo such as guns (Harmer, 2010a; Harmer, 2010b). But in these studies, target poles of various substances are extracted by using GPOF and results are given in the table. In this sense, these studies could not generate a solution about finding poles with GPOF mentioned above and could not demonstrate how much poles values changed with noisy signals.

Makal and his colleagues, have developed a method that uses wavelet transform and artificial neural network to distinguish cylindrical targets on the

infinite ground plane. Application of this method is given with noise analysis (Makal, 2008a; Makal, 2008b). However, for a proper training, especially when artificial neural networks used in target recognition applications many reference signals are required and it may not always be possible. Also, as a general problem of neural networks, whole educational process should be done from beginning in the case of adding a new target to database (even adding a new reference signal). Despite these disadvantages of the proposed methods, if wavelet coefficients of the signals are easily obtained, this method can be thought as an alternative way.

In the study of Chen and Shuley, PCA dimension reduction technique is successfully appllied to noiseless reference time scattering signals to find target poles (Chen and Shuley, 2008). But GPOF is used for target pole extraction again and the method could not be successful for noisy signals. However this study and also studies such as (Lee, 2008); (Huang, 2010a and Lee, 2010b), gave a supportive contribution for using dimension reduction techniques in this project.

E. Rothwell and his colleagues offered a frequency domain approach to the E-pulse radar target discrimination scheme. This approach is shown to allow easier interpretation of E-pulse convolutions via the E-pulse spectrum, and leads to a simplified calculation of pulse basis function amplitudes in the E-pulse expansion. Experimental evidence obtained using aircraft models verify the single-mode discrimination scheme, as well as the aspect-independent nature of the E-pulse technique. This leads to an integrated technique for target discrimination combining the E-pulse with single mode extraction waveforms.

As seen from literature generated studies have focused on finding target poles for noiseless signals. However, it is known that target poles are highly dependent on noise so noise test and results should be provided for studies examined above. In addition, although the target poles are extracted directly for noiseless signals, any information was not mentioned about how this knowledge can be used. The pulses generated in E-pulse method are very sensitive to pole values because of that pulses and classification performance quite change and the results of this state should be given for comparison with other methods.

As a result, it is thought that suggested methods and thesis outcomes can give a new contribution to high resolution and dimension reduction techniques in the target classification literature.

3 THE PROPOSED TARGET RECOGNITION WITH HIGH RESOLUTION TECHNIQUES

In this section, it is explained a development of a fast and sufficiently aspect-independent identification method with the processing of wideband scattered signals from radar targets. There are several methods which are explained in this section as ESPRIT, MUSIC and Min-Norm. However for the given method, ESPRIT (estimation of signal parameters by rotational invariance techniques) is mainly used for the classification stage of targets in resonance region. By using this technique, multiple reference vectors are reduced to one vector for each target with principal component analysis (PCA), and finally calculated vector is accepted as feature vector for the given target. Besides other dimension reduction techniques such as 'Average value method' and 'Common prediction matrix' are explained, however PCA technique is chosen for this suggested method since it gives best accuracy rates. The correlation coefficients of ESPRIT vectors between test signal and feature vector are compared for the classification phase and the one having highest correlation is assigned as the decision for the target.

3.1 High Resolution Techniques

When Fourier transform (FT) is applied to signal, local maxima are observed at about f_i values in radar cross section or scattered electric field figures. However, since FT has low resolution, high-resolution techniques such as MUSIC, ESPRIT are usually used, instead (Zhang, 2008; Gokalp, 2010; Lobos, 2010; Vasalos, 2011a; Vasalos, 2011b). These techniques are commonly used in direction-of-arrival and target detection applications. But when these techniques are used for finding pole values directly, they cause incorrect results in terms of real part of the pole at the high SNR values. So instead of finding pole values directly, these techniques aim to find classifiers as vectors, matrices etc. that contains indirect effects of pole values. In this part, to create a substructure about how to find damped sinusoidal signal parameters and vectors for the classification part will be explained with details for the ESPRIT (prediction of signal parameters), MUSIC and Min Norm methods.

11

3.1.1 **Music Algorithm and Music Spectrum Vector**

Late-time interval is given as shown in the following equation for noisy signal in the discrete time;

$$y(n) = x(n) + w(n) = \sum_{i=1}^{L/2} b_i \exp(-\alpha_i n \Delta t) \cos(2\pi f_i n \Delta t + \delta_i) + w(n), \quad n = 1,.., N \quad (3.1)$$

where w (n) is the noisy signal, L is the total number of damped exponentials and Δt is sampling period. Then covariance matrix of the discrete-time signal shown in (3.1) is estimated as follows:

$$\mathbf{R_{yy}} = \frac{1}{N} \sum_{n=m}^{N} \mathbf{Y}(n)^\mathrm{T} \mathbf{Y}(n), \quad \mathbf{Y}(n) = \begin{bmatrix} y(n) & \cdots & y(n-m+1) \end{bmatrix} \quad (3.2)$$

In this equation T symbolized the transpose operator and *m* is the MUSIC parameter and selected as N/2 for the best performance. Here matrix is separated into three different matices by using Singular Value Decomposition (SVD) with following equation.

$$\boldsymbol{R} = \boldsymbol{UDV}^H \quad (3.8)$$

In this expression, **U** and **V** are the unitary matrices for **R** matrix, and matrix **D** is the matrix whose diagonal elements contain the eigenvalues of matrix **R**. When these eigenvalues are put in order from highest to lowest as $\lambda_1 \geq \ldots \geq \lambda_L \geq \lambda_{L+1} \geq \ldots \geq \lambda_{m+1}$; vi belongs to the eigenvector of ith eigenvalue. In this way, v_i vectors which are belong to eigenvalues $\lambda_1 \geq \ldots \geq \lambda_L$ for i = 1,...,L cover the signal subspace, v_i vectors which are belong to eigenvalues $\lambda_{L+1} \geq \ldots \geq \lambda_{m+1}$ for i = L+1,...,m+1 cover the noise subspace.

Then using covariance matrix in frequency domain, MUSIC spectrum vector is calculate in this way;

$$\mathbf{P_{MUSIC}} = \begin{bmatrix} P(f_1) & P(f_2) & \cdots & P(f_s) \end{bmatrix} \quad (3.3)$$

$$P(f) = \frac{1}{\sum_{k=L+1}^{m} \left| \mathbf{v_k^T} \mathbf{e}(f) \right|^2}$$

(3.4)

$$\mathbf{e}(f) = \begin{bmatrix} 1 & \exp(-j2\pi f \Delta t) & \cdots & \exp\left[-j2\pi f(m-1)\Delta t\right] \end{bmatrix}^{\mathrm{T}}$$

(3.5)

where s is the number of sample frequency number and $\mathbf{v_k}$ is the kth right eigenvector of $\mathbf{R_{yy}}$ matrix when singular value decomposition (SVD) is applied. MUSIC spectrum vector in equation (3.3) give the peak values on the f_i frequencies if the signal is in the form of summation of noiseless undamped sinusoidal waves and otherwise MUSIC spectrum vector gives approximate peak values on the f_i frequencies if the signal is in the form of summation of sine waves with decreasing amplitudes as shown in the equation (3.1).

3.1.2 **Min-Norm Algorithm and Min-Norm Spectrum Vector**

If we want to express the expression in equation (3) in other way in the discrete time region;

$$y(n) = \sum_{i=1}^{L} c_i e^{s_i n \Delta t} + w(n), \qquad n = 0, \ldots, N$$

(3.6)

The signal in equation (3.6) is not stable and operates in the complex frequency region instead of real frequency region so instead of using covariance matrix calculated in Min-Norm method, alternatively a prediction matrix can be used that dimensions are (N-m+1) x (m+1) as given below;

$$\boldsymbol{R} = \begin{bmatrix} y(0) & y(1) & \cdots & y(m) \\ y(1) & y(2) & \cdots & y(m+1) \\ \vdots & \vdots & \ddots & \vdots \\ y(N-m) & y(N-m+1) & \cdots & y(N) \end{bmatrix}$$

(3.7)

where m is Min-norm parameter and for the best performance, m is chosen as $N / 2$. Singularity Expansion Method is used to find eigenvectors which is demonstrated previously.

13

Eigenvectors, which cover the noise subspace are expressed as follows;

$$G = \begin{bmatrix} v_{L+1} & \cdots & \cdots & v_{m+1} \end{bmatrix} = \begin{bmatrix} \beta \\ G_1 \end{bmatrix} \tag{3.9}$$

where β vector is the first row vector of the **G** matrix. In Min-Norm method, instead of using all vectors in **G** matrix, only one vector is used similarly as expressed in MUSIC algorithm. By this way a significant computational reduction is obtained. This vector is pointed out as indicated in equation (3.10);

$$g = \begin{bmatrix} 1 \\ G_1 \beta^H / \|\beta\|^2 \end{bmatrix} \tag{3.10}$$

where $\| \cdot \|$ and H are respectively the norm and Hermitian operators. As a last step, target poles belong to a target reference signal are calculated as the roots of the following equation.

$$a^H (s) g = 0 \tag{3.11}$$

$$a(s) = \frac{\begin{bmatrix} 1 & e^{-s\Delta t} & e^{-2s\Delta t} & \cdots & e^{-ms\Delta t} \end{bmatrix}^T}{\left\| \begin{bmatrix} 1 & e^{-s\Delta t} & e^{-2s\Delta t} & \cdots & e^{-ms\Delta t} \end{bmatrix} \right\|} \tag{3.12}$$

The neglected denominator part of the equation (3.12) for undamped sinusoidal waves has been replaced by the proposed method as a critical modification for damped sine signals. Similar to MUSIC algorithm, by using equation (3.10) Min-Norm vector is given as follows in frequency domain;

$$F = \begin{bmatrix} \dfrac{1}{\|g^T e(f_1)\|} & \dfrac{1}{\|g^T e(f_2)\|} & \cdots & \cdots & \dfrac{1}{\|g^T e(f_s)\|} \end{bmatrix} \tag{3.13}$$

where T symbolized the operator of transpose function, s is the number of frequency samples as f_1, f_2 ,..., f_s and **e**(*f*) is as expressed in equation (3.5). According to

orthogonality principle in Min-norm method, $g^T e(f)$ has minima values at $f = f_i$ frequencies because of that the vector in the equation (3.13) should give peak values at approximately f_i frequencies.

3.1.3 **ESPRIT Algorithm and ESPRIT Spectrum Vector**

ESPRIT method uses the formula (3.1) and creates a prediction matrix as shown in the formula (3.2). Then subspace vectors are created by using singularity expansion method. Eigenvectors of signal subspace are summed as given in the matrice shown below equation for i = 1, ..., L

$$\mathbf{S} = \begin{bmatrix} \boldsymbol{e_1} & . & . & . & \boldsymbol{e_L} \end{bmatrix} \tag{3.14}$$

According to the ESPRIT method, by using given matrix, two auxiliary matrices can be defined as;

$$\mathbf{S_1} = \begin{bmatrix} \mathbf{I}_{m \times m} & \mathbf{0} \end{bmatrix} \mathbf{S} \tag{3.15}$$

$$\mathbf{S_2} = \begin{bmatrix} \mathbf{0} & \mathbf{I}_{m \times m} \end{bmatrix} \mathbf{S} \tag{3.16}$$

where $\mathbf{I}_{mxm}$ is the unit matrix, which has the size of $\mathbf{m \times m}$. $\mathbf{0}$ vector is an m-element column vector, whose element values are all zero. According to ESPRIT algorithm, the arguments of eigenvalues of $\boldsymbol{\psi}$ matrix given in equation below, are complex s_i values of the given target.

$$\mathbf{S}_2 = \mathbf{S}_1 \boldsymbol{\psi} \tag{3.17}$$

This $\boldsymbol{\Psi}$ matrix is calculated as follows using the least squares estimation:

$$\boldsymbol{\psi} = (\mathbf{S}_1^H \mathbf{S}_1)^{-1} \mathbf{S}_1^H \mathbf{S}_2 \tag{3.18}$$

ESPRIT method is more preferable technique when it is compared to other methods because usually ESPRIT has less sensitivity to noise. After pole extraction, equation is shown that uses pole informations in case of creating ESPRIT spectrum vector;

$$P(z) = \det(z\mathbf{I}_{L \times L} - \boldsymbol{\psi}) = \prod_{i=1}^{L/2}(z - z_i)(z - z_i^*) = z^L + a_1 z^{L-1} + \ldots + a_{L-1}z + a_L$$

(3.19)

where $z_i = \exp(s_i \Delta t)$. Then, by giving ai values of given equation above in a vectorial form as $\boldsymbol{a_{esp}} = [1 \quad a_1 \quad \ldots \quad a_{L\text{-}1} \quad a_L]$, the ESPRIT spectrum function for this sample signal is defined by

$$P(f) = \frac{1}{\left| \boldsymbol{a}_{esp} \boldsymbol{e}(f) \right|}$$

(3.20)

$$\boldsymbol{a}_{esp} = \begin{bmatrix} 1 & a_1 & \ldots & a_{L-1} & a_L \end{bmatrix}$$

(3.21)

$$\boldsymbol{e}(f) = \begin{bmatrix} 1 & e^{-j2\pi f \Delta t} & \cdots & e^{-j2\pi fL\Delta t} \end{bmatrix}^T$$

(3.22)

Finally, ESPRIT spectrum vector is obtained by taking samples from the function in (3.20) at the desired discrete frequency points. It should be noted that since $F(z)$ has zeros at $z_i = e^{s_i \Delta t} = e^{(-\alpha_i \pm j2\pi f_i)\Delta t}$, this ESPRIT vector has local maxima at about $f = f_i$ values, which are specific to the target. Those signals are not stable because of being damped sine waves and in this sense instead of defining as power spectrum, can be defined as amplitude spectrum (Stoica and Moses, 2005). Similarly to radar cross section area, this function also should give local maxima values at $f = f_i$.

Finally ESPRIT spectrum vector is defined by sampling the R number discrete frequencies as given;

$$\boldsymbol{P} = \begin{bmatrix} P(f_1) & P(f_2) & \ldots & P(f_R) \end{bmatrix}$$

(3.23)

3.2 Dimension Reduction Techniques

In feature extraction stage of target classification, usually several reference scattering signal is used for each target. After processing this signal with high-resolution techniques, feature vectors are obtained as number of reference signal for each target. Because of that in target classification methods, generally an attempt is made to reduce the number of feature vectors to one vector for each target with

16

dimension reduction techniques. Choosing just one vector for each target by combining the effects of all reference ESPRIT vectors significantly decreases computational time and memory storage.

3.2.1 **Principal Component Analysis**

Firstly, this method was introduced by Pearson and it is widely used for data compression and dimension reduction techniques (Jackson, 1991). The PCA dimension reduction technique is used to obtain a feature vector for each target, which becomes highly correlated with corresponding K different ESPRIT spectrum vectors. By assuming that all reference ESPRIT spectrum vectors of a target are row vectors with s-elements (s is the number of frequency samples), the matrix G can be defined as;

$$G = \begin{pmatrix} P_{ESPRIT,1} - mean(P_{ESPRIT,1})1_{1 \times S} \\ P_{ESPRIT,2} - mean(P_{ESPRIT,2})1_{1 \times S} \\ \vdots \\ P_{ESPRIT,K} - mean(P_{ESPRIT,K})1_{1 \times S} \end{pmatrix} = \begin{pmatrix} G_1 \\ G_2 \\ \vdots \\ G_K \end{pmatrix} \tag{3.24}$$

where $P_{ESPRIT,i}$ for i = 1, 2, …, K is the normalized ESPRIT spectrum vector of ith aspect angle and $1_{1 \times s}$ is the row vector whose elements are equal to one. Then, the matrix of **C** is defined as the covariance matrix of **G** in the general form;

$$C = \begin{pmatrix} c_{11} & c_{12} & \cdots & c_{1K} \\ c_{21} & c_{22} & \cdots & \vdots \\ \vdots & \vdots & \ddots & \vdots \\ c_{K1} & c_{K2} & \cdots & c_{KK} \end{pmatrix} \tag{3.25}$$

where c_{ij} defines the covariance between vectors G_i and G_j. The principal component row vectors (z_1, z_2, ..., z_K) are calculated by via **C** matrix as

$$\begin{pmatrix} z_1 \\ z_2 \\ \vdots \\ z_K \end{pmatrix} = U^T G, \quad U = \begin{bmatrix} u_1 & u_2 & \cdots & u_K \end{bmatrix} \tag{3.26}$$

17

where u_1, u_2, ..., u_K are normalized column eigenvectors of matrix $\mathbf{C}$ corresponding to the eigenvalues arranged in non-increasing order as $\lambda_1 \geq \lambda_2 \geq \ldots \geq \lambda_K$. Eventually, the feature vector $\mathbf{F}$ for this target is constituted as

$$F = \frac{\sum_{i=1}^{K} \lambda_i z_i}{\sum_{i=1}^{K} \lambda_i}$$

(3.27)

which includes the contributions from all principal component vectors. However, if the percentage of λ_1 in the summation of eigenvalues (λ_1 values) is sufficiently large (for instance, higher than 90%), the other principal components can be neglected and the feature vector F becomes equal to first principal component z_1 only. However, the contributions of other components should be considered if the percentage of first component is inadequate. The mentioned steps so far for the extraction of feature vector of a single target are repeated for each known target and a total of M feature vectors for M targets are stored to feature database.

3.2.2 Average Value Method

This technique can be defined as classic "average value" method. Average value method is based on normalizing spectrum vectors for K different reference signal of a target and taking the average value at each frequency point.

$$\mathbf{F} = \frac{\sum_{i=1}^{K} \mathbf{P_{norm,i}}}{K}$$

(3.28)

$$P_{norm,i} = \frac{[P(f_1) \quad P(f_2) \quad \ldots \quad P(f_R)]}{\left\| [P(f_1) \quad P(f_2) \quad \ldots \quad P(f_R)] \right\|}$$

(3.29)

18

3.2.3 **Common Prediction Matrix**

In the mentioned techniques as ESPRIT, spectrum vector creation process is belong to single reference signal and this process should be executed K times for K number reference signals for each target. The matrix which is shown below is created over again. After that, other steps are applied separately for each time and K number spectrum vectors are obtained. Then by using dimension reduction techniques which are discussed in previous sections, obtaining a single feature vector from K number different vectors are tried. But this situation can cause a significant increase in calculation time when there are many reference numbers. So instead of creating new matrices over and over again, one single common prediction matrix is created which is fused the effects of all reference scattering signals. This matrix equation is defined as shown below and the dimensions are K(N-m+1) and (m+1). This method also can be thought as dimension reduction technique;

$$
R = \begin{bmatrix} y(0) & y(1) & \cdots & y(m) \\ y(1) & y(2) & \cdots & y(m+1) \\ \vdots & \vdots & \ddots & \vdots \\ y(N-m) & y(N-m+1) & \cdots & y(N) \end{bmatrix} \tag{3.30}
$$

$$
R = \begin{bmatrix} y_1(0) & y_1(1) & \cdots & y_1(N-m) & y_2(0) & y_2(1) & \cdots \\ y_1(1) & y_1(2) & \cdots & y_1(N-m+1) & y_2(1) & y_2(2) & \cdots \\ \vdots & \vdots & \ddots & \vdots & \vdots & \vdots & \ddots \\ y_1(m) & y_1(m+1) & \cdots & y_1(N) & y_2(m) & y_2(m+1) & \cdots \end{bmatrix}
$$
$$
\begin{bmatrix} y_2(N-m) & \cdots & y_K(0) & y_K(1) & \cdots & y_K(N-m) \\ y_2(N-m+1) & \cdots & y_K(1) & y_K(2) & \cdots & y_K(N-m+1) \\ \vdots & \cdots & \vdots & \vdots & \ddots & \vdots \\ y_2(N) & \cdots & y_K(m) & y_K(m+1) & \cdots & y_K(N) \end{bmatrix}^T \tag{3.31}
$$

Then applying the other steps described in the high-resolution techniques, spectrum vector is calculated. In the matrix shown in the equation (3.31) has m+1 columns because of this resulting right eigenvector matrix after SVD, has m+1 columns too. Therefore, there is no need for any modification at the remain part of the method.

19

3.3 Steps of Radar Target Classification Method and Flowchart

In this part of the thesis, radar target classification steps will be explained. Similar to other resonance scattering region methods, in suggested study based on Singularity Expansion Method, materials and tehniques are discussed above. Here, steps of this suggested method which is the combination of techniques and materials may be expressed briefly as follows:
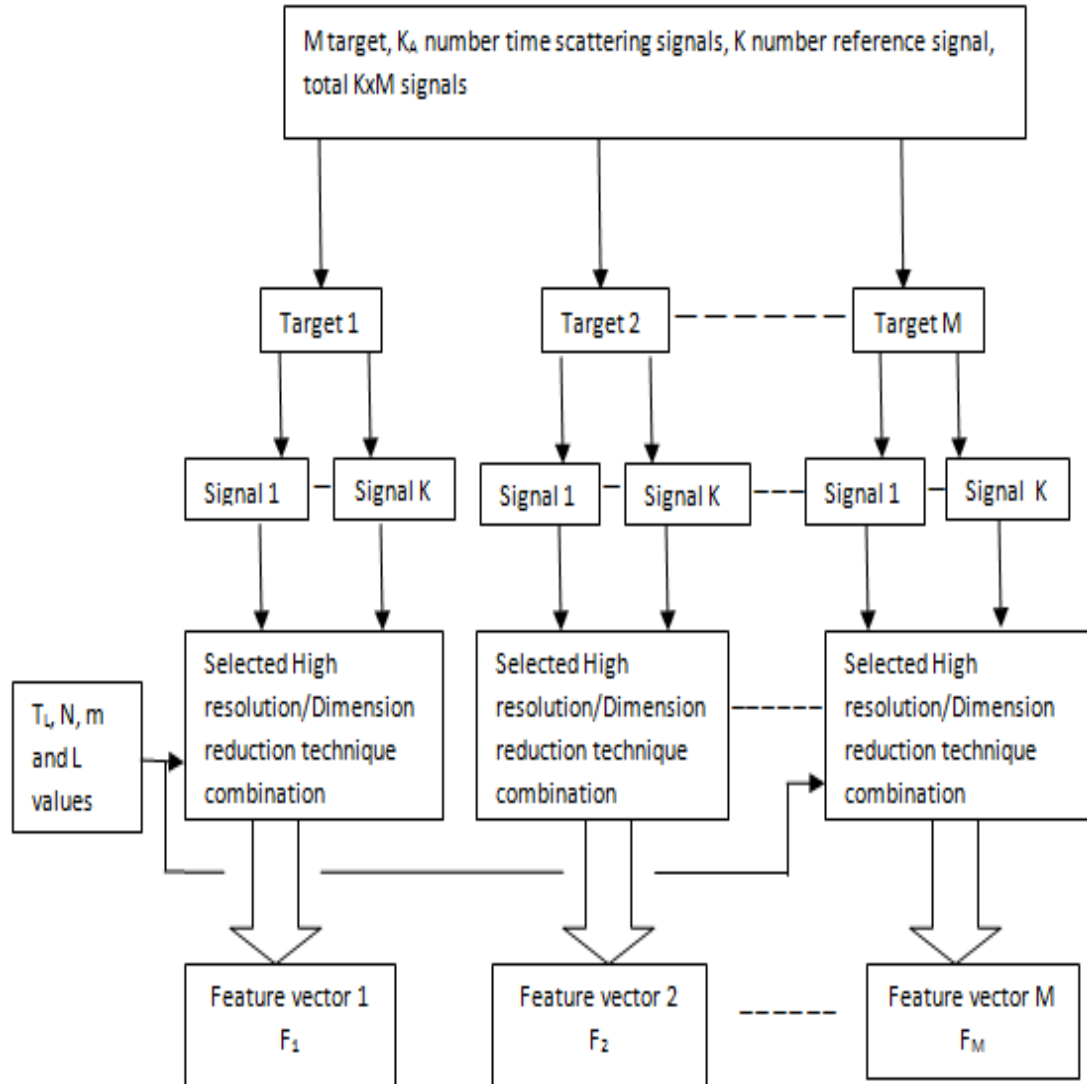
i)   In the formation of suggested method, it is assumed to be M targets each having K scattered signals of different aspect angles, which gives a total of K×M reference signals. Lets suppose that scattering datas for this case are obtained as time signals. Thus, equation of scattering time signal becomes as equation (2). Here K number reference signals from K_A different signals which gives a total of $K_A \times M$ reference scattering signals. When resonance region scattering property is thought differences between reference angles should be at least 10-15 degrees.

ii)   A late time scattering point is determined for all time scattering signals. Defining starting point and late time interval may be done in several ways as discussed in some studies (Turhan-Sayan, 2005; Secmen, 2008) but in suggested method similarly to methods in literature, common starting point can be calculated as $T_L = T_P + 2T_D$. Here, T_P is the width of the pulses that sent to the target and easily calculated from frequency band, T_D is calculated from $T_D = L_{max} / c$ (c:speed of light). In this equation L_{max} is the longest line of biggest target in the target set.

iii)   After defining common late-time starting point, late time interval is determined. At this step, N is selected 64, 128, 256 (time sample) as square of 2 in many cases in late time interval to make the code of method faster. As related to high resolution techniques m parameter is chosen N/2. L parameter which determines the pole numbers for a signal is chosen as common for all signals or is calculated different for all signals with minimum description length (minimum description length-MDL) method.

iv)   After selecting all the parameters described above, one of the high resolution techniques and one of the dimension reduction techniques are

chosen. Target specific feature spectrum vector is extracted by applying resolution/dimension reduction combination to the late-time interval which is belong to reference signals of a target. This process is applied to all targets and spectrum vectors are obtained. Let these feature vectors become F_i (i = 1, 2, ..., M).

v)   Let we assume that a test target, in classification or the testing phase which is actually one of the candidates but in test stage we do not know which one is. Also it is supposed a scattering signal belong to any angle condition. This test scattering signal can be noisy or noiseless in real-life applications. Parameters of mentioned above is applied with a high resolution technique and test spectrum vector, P_{test}, is obtained. Test target is one of the known targets so according to Singularity Expansion Method the position of the peak frequency in the test spectrum vector should be close to the related candidate target peak frequency. With the same approach peak frequency must be different from others. Thus it is expected that correlation coefficient should be high between ESPRIT vector and candidate target and should be low with other targets. For this purpose, test vector and feature vectors (F_i (i = 1, 2, ..., M)) are compared with a simple correlation coefficient calculation.

$$r(i) = \frac{\bar{P}_{test} F_i^T}{\left|\bar{P}_{test}\right|\left|F_i\right|} \quad i = 1, 2, ..., M \quad \bar{P}_{test} = P_{test} - mean(P_{test})I_R \qquad (3.32)$$

Here $\left|.\right|$ is norm operator, F_i is the feature vector for candidate target, $r(i)$ is the correlation coeffcient between P_{test} and F_i vectors. Finally with the equation (3.32), test target in the proposed target classificiaton method, is classified as the target that gives the highest correlation coefficient rate. Flow charts, steps, extracting feature vectors stages and test stages of the proposed radar target classification method described so far shown seperately in Fig 3.1 and Fig 3.2, respectively.

```
┌────────────────────────────────────────────────────────────────────┐
│ M target, K_A number time scattering signals, K number reference     │
│ signal, total KxM signals                                            │
└────────────────────────────────────────────────────────────────────┘
```

M target, K_A number time scattering signals, K number reference signal, total KxM signals

| Target 1 | Target 2 | - - - - - | Target M |

| Signal 1 | Signal K | | Signal 1 | Signal K | - - - | Signal 1 | Signal K |

| T_L, N, m and L values |

| Selected High resolution/Dimension reduction technique combination | Selected High resolution/Dimension reduction technique combination | - - - - - | Selected High resolution/Dimension reduction technique combination |

| Feature vector 1 F_1 | Feature vector 2 F_2 | - - - - - | Feature vector M F_M |

Figure 3.1 Flow chart for the feature vectors extraction stage for proposed method
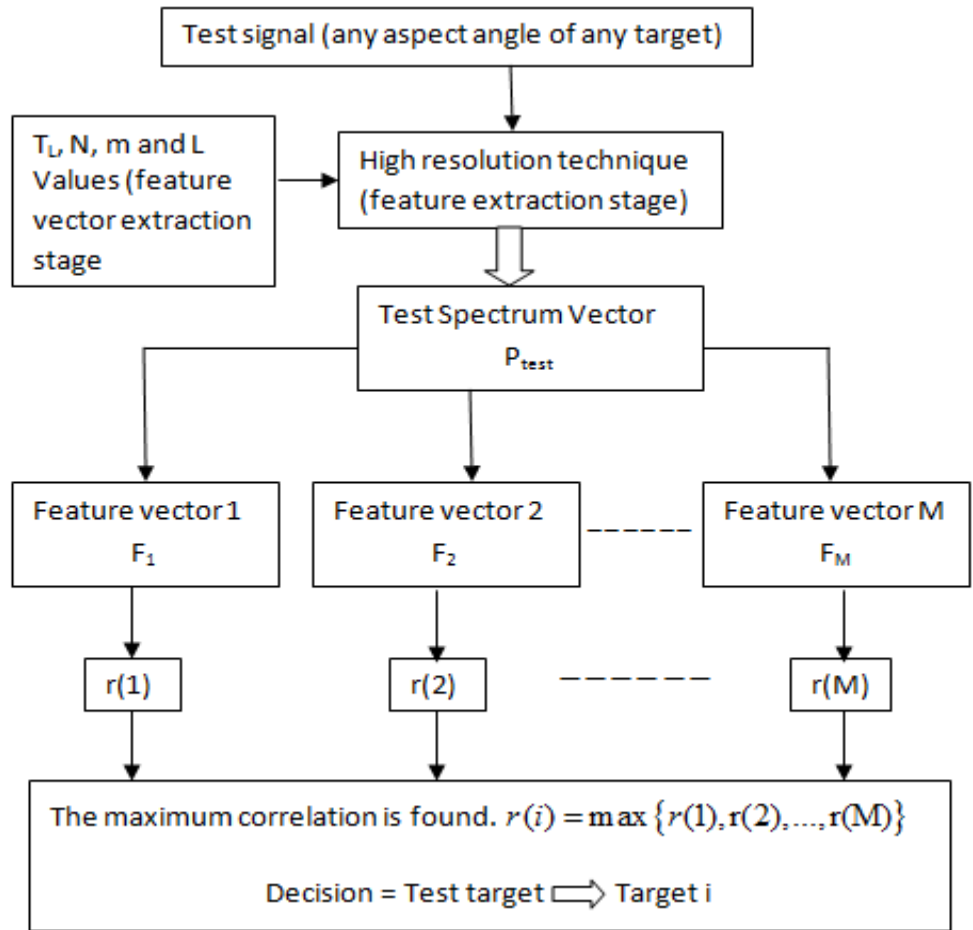
Figure 3.2 Flow chart for the test stage of proposed method

4   APPLICATION AND RESULTS FOR HOGH RESOLUTION TECHNIQUES

Small-scale airplane targets (Airbus, Boeing 747, Caravelle and Tu-154) modeled with thin, straight, conducting wires are used for the suggested method. Dimensions and geometrical structure are shown below in Table 4.1. and Figure 4.1.

**Table 4.1 The Dimensions of the Airplane Targets in Meters**

Structures	Airplane Targets			
	Airbus	*Boeing 747*	*Caravelle*	*Tu-154*
Body (m)	0.5408	0.7066	0.3200	0.4790
Wing (m)	0.4484	0.5964	0.3440	0.3755
Tail (m)	0.1626	0.2217	0.1092	0.1340

(a)   (b)
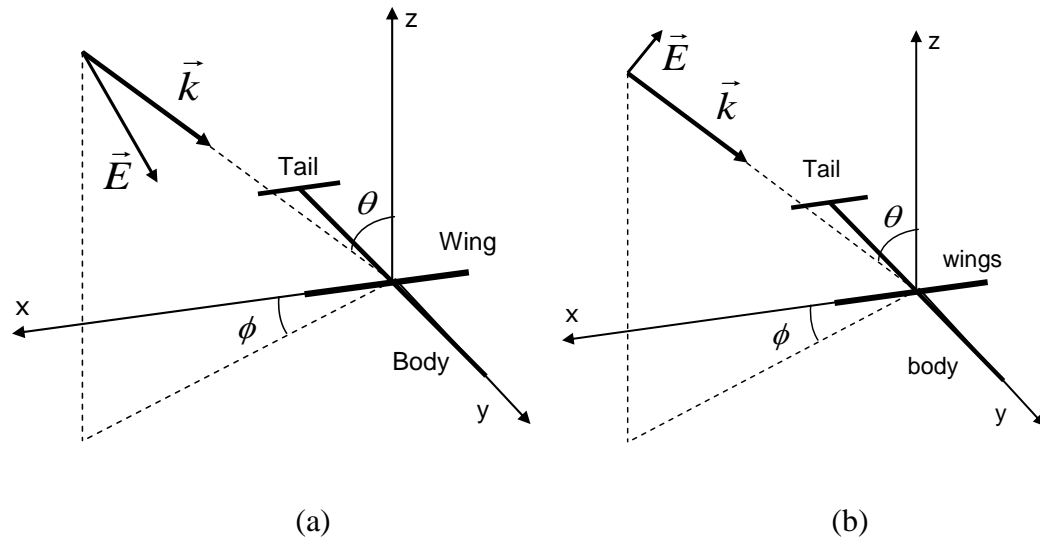
Figure 4.1 Geometrical structure for the application. (a) ϕ polarization (b) θ polarization

The backscattered (monostatic) frequency responses of all targets are generated by using CST Microwave Studio for a fixed elevation angle θ = 60° and linear polarization in Φ direction for both incident and scattered fields as shown in Figure 4.1(a). Scattered fields are obtained for several azimuth angles at Φ = 0°, 2.5°, 5°, …,

24

87.5°, 90° (a total of 37 azimuth angles). The frequency bandwidth of the responses is 4–1024 MHz. When the dimensions of the targets are considered, all targets are said to be safely in resonance scattering region that the largest dimension, body length of Boeing 747 (0.7066 m), is at most 2.4λ for the given frequency bandwidth and resolution value of 4 MHz. Time resolution is calculated as 500 ps. The resulting frequency responses are converted from frequency domain to time domain by using Gaussian window and inverse FFT. As a sample two time domain scattered signals are plotted for Airbus and Tu-154 airplanes at $\phi = 30°$ in Figure 4.2.
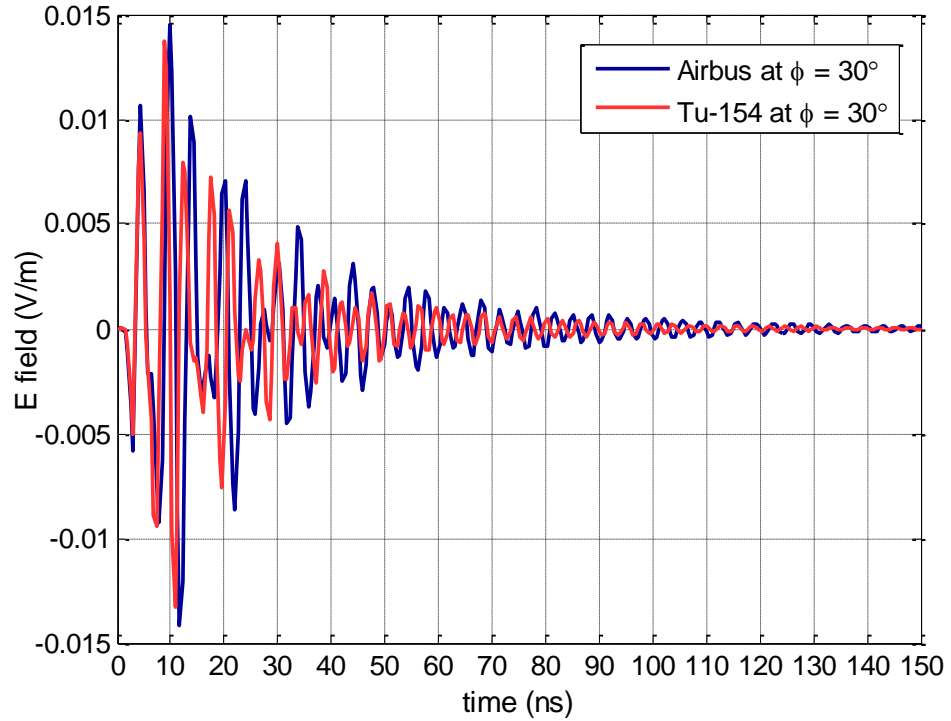

Figure 4.2 Time-domain scattered signals for Airbus and Tu-154 airplane targets at $\phi = 30°$.

The reference signals for the construction of feature vectors are selected as time responses coming from only 5 aspect angles ($\phi = 5°$, 22.5°, 45°, 67.5° and 85°) out of 37 aspect angles for each target. Next, the late-time portions of these signals are considered for the following steps. As explained before, the late-time portion of the signals starts after the incident wave has no influence on the target. By using this definition, the start time instant can be approximated as $T_{start} = T_p + 2T_d$, where T_p is the pulse duration (about 1 ns in this application) and T_d is the duration for the incident wave to fully pass the target (Rothwell, 1994). In this application, for the sake of guarantee, T_d is selected as its highest value for all signals, which is equal to

25

$T_d = D_{max}/c$, where D_{max} is the longest linear dimension for all airplane targets and c is the speed of light. D_{max} corresponds to the diagonal dimension of Boeing 747, which has the longest body and wing dimensions among all targets. Therefore, T_d is approximately evaluated as 3 ns and T_{start} is calculated as 7 ns.

So time instants for late time signals is chosen as 7 ns and $N = 64$ time samples. Here while getting feature vectors with PCA, ESPRIT parameter is selected $m = N / 2 = 32$ and $L = 6$ for the best accuracy performance. In Figure 4.3 feature vector for each target is demonstrated. This step was also repeated for different L values such as $L= 4$ and $L=8$ except $L=6$. However, $L=6$ gives the best performance among these values.
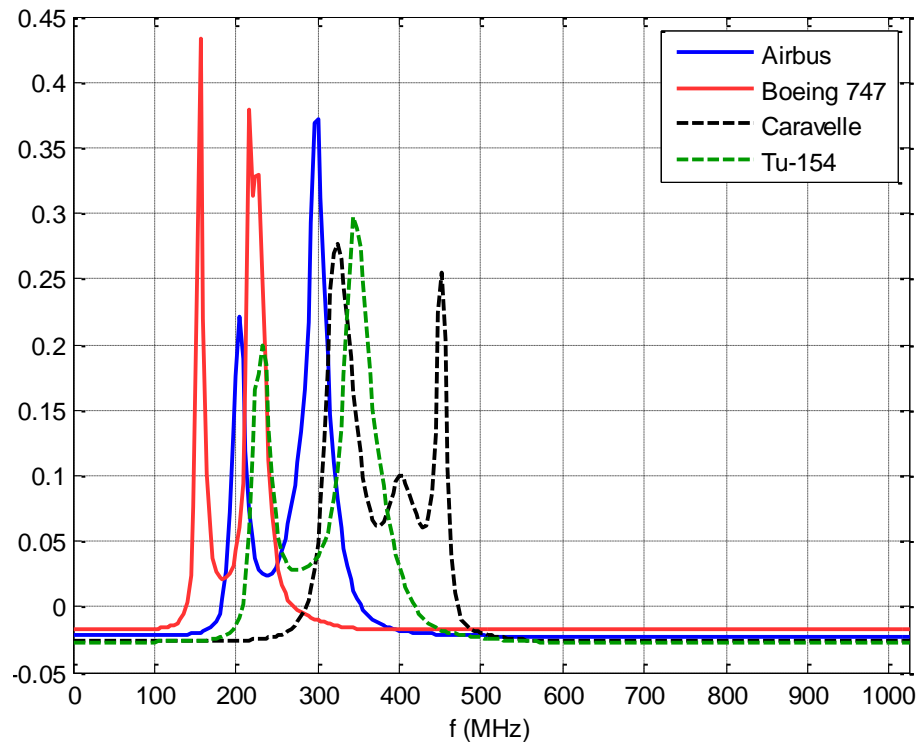
**Figure 4.3 The feature vectors of the airplane targets in the demonstration.**

Table 4.2 Identification rates for different L values

L	PCA	Common Prediction Matrix	Averaging Value Method
4	94.32	94.59	70.94
6	100	95.27	87.83
8	94.32	99.32	85.81

In classification stage of the proposed method is executed with 37 signal $\times$ 4 target = 148 test signals. While attaining test ESPRIT spectrum vectors, same late-time intervals and parameters (N = 64, m = 32 and L = 6) are used. For this step inially noiseless signals are considered. The correlation coefficients are calculated with the equation below;

$$r(i) = \mathbf{P}_{\text{test}}\mathbf{F}_{\mathbf{i}}^{\text{T}}\Big/\Big(\big|\mathbf{P}_{\text{test}}\big|\big|\mathbf{F}_{\mathbf{i}}\big|\Big), \quad i = 1,\ldots,M \tag{4.1}$$

Then according to highest correlation coeffcients, comparison between test vector and target feature vectors one by one, give us the decision about test target. For instance, for a test signal of Airbus airplane at the angle of $\phi = 30°$, whose time-domain signal is given in Fig. 4.4, the resulting test ESPRIT vector is plotted in Fig. 4.4. Then correlation coefficients are obtained by the help of spectrum vector which is shown previously for Airbus, Boeing 747, Caravelle and Tu-154 as 0.9430, 0.2056, 0.0628 and 0.1819, respectively.
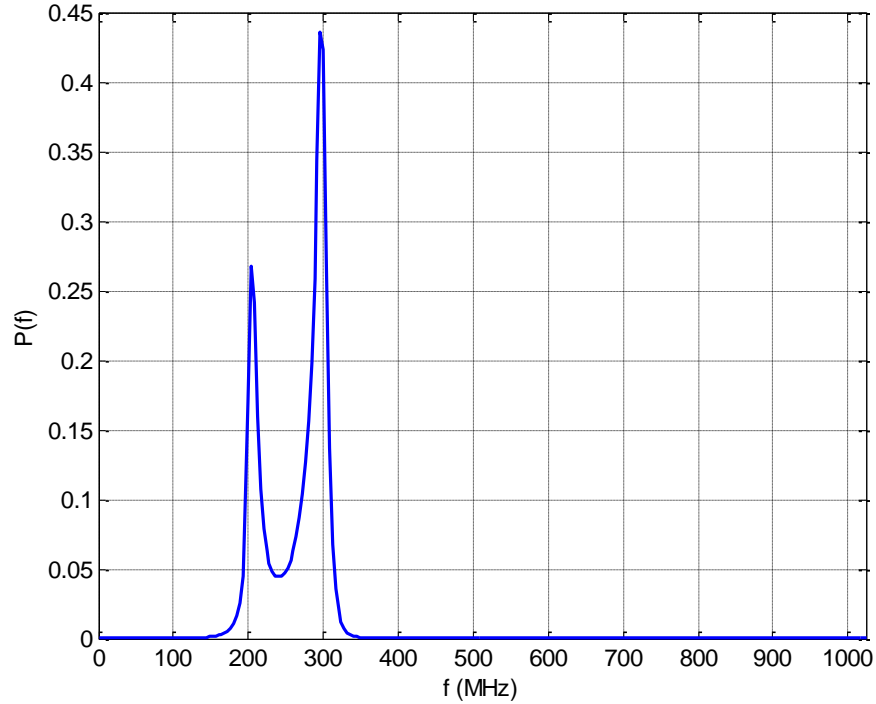
Figure 4.4 Test ESPRIT spectrum vector for the scattered signal of Airbus airplane target at $\phi =$ 30°.

According to figures, after having comparisons and calculations it can be found with high accuracy rates that test target is Airbus. When all scattering signals (148 signals) are considered with the same test approach, the correct identification rate is found to be 100 percent for this target set application that all test targets are regularly identified.

As a secondary test noisy signals are generated and implemented to demonstrate noisy performance of suggested method. Zero-mean Gaussian noise is used to create noisy signals with signal-to-noise (SNR) levels values of 20, 15, 10, 5, 0, -2.5 and -5 dB. 100 independent trials for each SNR level are performed to reduce the dependency of the results on noisy statistics. The corresponding correct identification rates (in percentage) for both noiseless and noisy cases are given in the first row of Table 4.3.

28

Table 4.3 The Correct Identification Rates of The Application with PCA and Other Dimension Reduction Techniques

Dimension Reduction Technique	SNR (dB)							
	∞	*20*	*15*	*10*	*5*	*0*	*-2.5*	*-5*
PCA	100	99.94	99.77	99.5	98.74	96.09	93.6	88.31
Averaging	99.32	98.94	98.81	97.76	95.37	91.01	88.32	84.01
CPM	87.83	87.11	86.48	85.35	83.99	81.68	79.44	76.15

As shown from these results, the proposed identification method can give higher than 88 percent accuracy even for very noisy signal level of SNR = -5 dB, which is quite high and satisfactory for target identification applications. To show the effectiveness of the PCA technique implemented in the proposed method, the simulations of the given application are repeated with some other dimension reduction techniques instead of PCA. The realized techniques are the classical averaging, which summons all normalized reference ESPRIT spectrum vectors of a target and divides the resulting vector by 4, and common prediction matrix (CPM) method whose details can be found in (Secmen M., 2012). They are used to obtain the related feature vectors from reference vectors, and the tests are performed in a same way explained above. The corresponding results are given in Table 4.3 and Figure 4.5, and PCA technique is shown to be superior at all SNR levels.
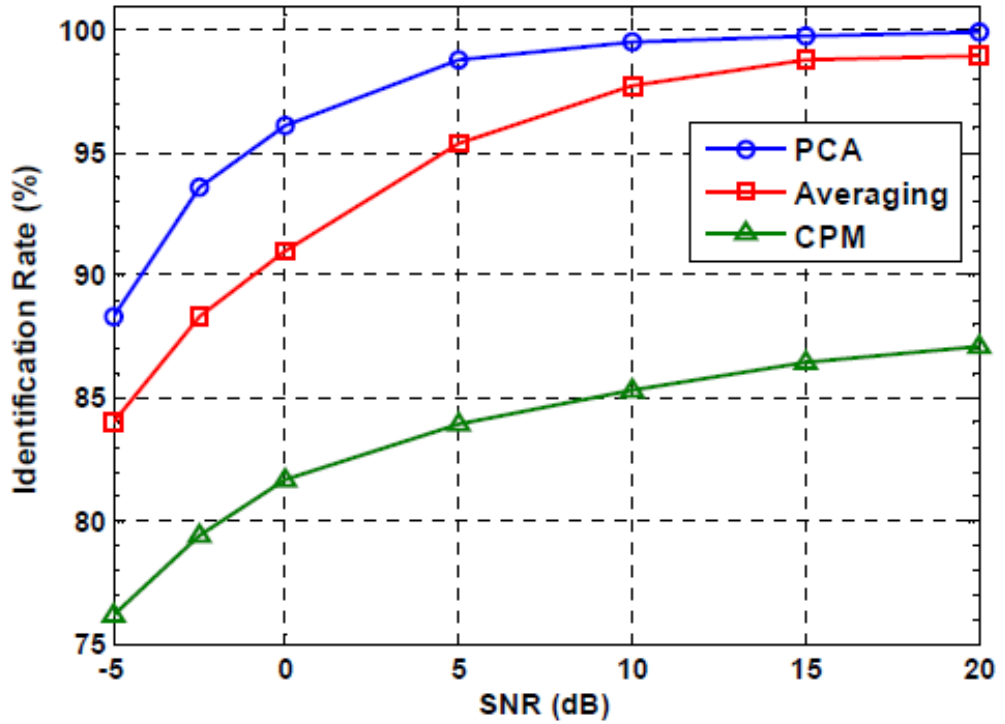
Figure 4.5 The correct identification rates of the given application with PCA and other dimension reduction techniques.

In order to compare and show the performances of the different high-resolution techniques such as ESPRIT, MUSIC, Min-Norm as well as FFT, a new classifier is designed. In this analysis, as being different than the previous configuration, which belongs to the configuration in Figure 4.1(a), the configuration in Figure 4.1(b) is used. The configuration in Figure 4.1(a) differs from the one in Figure 4.1(b) only in terms of the polarization of the incident and scattered waves. Therefore, with this test scenario, it is also aimed to observe the independency of the proposed method to the polarization changes. In the calculations and simulations of the mentioned scenario, all targets, angles, values and parameter values are kept constant with the previous scenario (the one with Figure 4.1(a)). Table 4.4 shows the corresponding results (accuracy rates) and the performance comparison between ESPRIT, MUSIC, Min-Norm and FFT algorithms. While getting these accuracy rates, the dimension reduction of PCA is used for all algorithms. When the results in Table 4.4 are examined, it can be said that ESPRIT possesses the highest correct classification rates as compared to other algorithms by giving the percentages of 93.2, 97.8, 98.8, 99, 99.3, 99.8 for the SNR values 0, 5, 10, 15, 20, 25 dB, respectively. Besides, it can be

30

observed in this scenario that the proposed classification method consisting of ESPRIT algorithm and PCA technique has similar (and again satisfactory) accuracy rates with the previous case (the one with different polarization). Therefore, it can be concluded that the proposed method is highly independent from polarization of the scattered signals.

Table 4.4 Performance comparisons between High Resolution Techniques

Strategy	SNR (dB)					
	25	20	15	10	5	0
ESPRIT	99.8	99.3	99	98.8	97.8	93.2
MUSIC	96.9	97.1	95	87.6	81.3	79.5
MIN-NORM	98.3	98.1	95	89	86.2	84.9
FFT	69.7	69.4	69	67.9	66.7	66

As being another crucial criterion in target identification applications, the decision-time for a test target is also computed. A typical decision takes only 8 ms in MATLAB environment with a computer having microprocessor of Intel Core i7, 3.06 GHz, which is fast enough for real-time applications.

5   THE PROPOSED TARGET RECOGNITION WITH TIME FREQUENCY REPRESENTATIONS

In the literature, some studies such as (Chen and Shuley) and (Turhan Sayan, 2005) apply TFR's techniques to classify targets such as dielectric spheres which have several poles. Here it is intended to develop these studies and Wigner Ville method with "target specific" and "signal specific" strategies are examined for this reason.

This study aims to have reduction on target's distance, aspect angle and noise dependencies for the target classification method in resonance region. In the given method, crucial optimum late-time intervals of the scattered signals are determined by using time-frequency representations. The maximum and mean power values are used as time instants which are independent from targets position in the time-frequency distributions. Then, the feature vectors are formed for each target by using the given time-frequency distributions over these selected late-time regions at several different reference aspects, and they are eventually used for the classification in test stage. In this work, two different strategies are designed; target-specific and signal-specific late-time intervals. The simulations are carried out with lossless dielectric spheres being challenging targets in terms of scattering mechanism. Also in this stage the performances are explained and compared for different popular time-frequency representations in the literature as Page, STFT and Wigner-Wille methods.

5.1   Wigner-Wille Method

In this study, Wigner Ville Distribution is employed in order to determine the target responses. The reasons of choosing the Wigner Ville Distribution are that WD can provide best time and frequency resolution and WD supplies the large number of mathematical properties. WVD always preserves the time and frequency shifts and respectively corresponds to the signal's instantaneous power and its spectral energy density. The purpose of the energy distributions is to distribute the energy of the signal over the two description variables: time and frequency. As the energy is a quadratic function of the signal, WVD will be in general quadratic representation. The Wigner- Ville energy distribution in terms of the signal, $x(t)$ or its spectrum $X(w)$ is defined by;

$$W_x(t, f) = \int_{-\infty}^{+\infty} x(t + \frac{\tau}{2}) x*(t - \frac{\tau}{2}) e^{-j2\pi f\tau} d\tau \tag{5.1}$$

or equivalently by;

$$W_x(t, f) = \int_{-\infty}^{+\infty} X(f + \frac{\varepsilon}{2}) X*(f - \frac{\varepsilon}{2}) e^{-j2\pi\varepsilon\tau} d\varepsilon \tag{5.2}$$

A sample signal and Wigner distributions of the sample signal are given in the Figure 5.1 for $\varepsilon_r = 3$ and $\theta = 179°$.
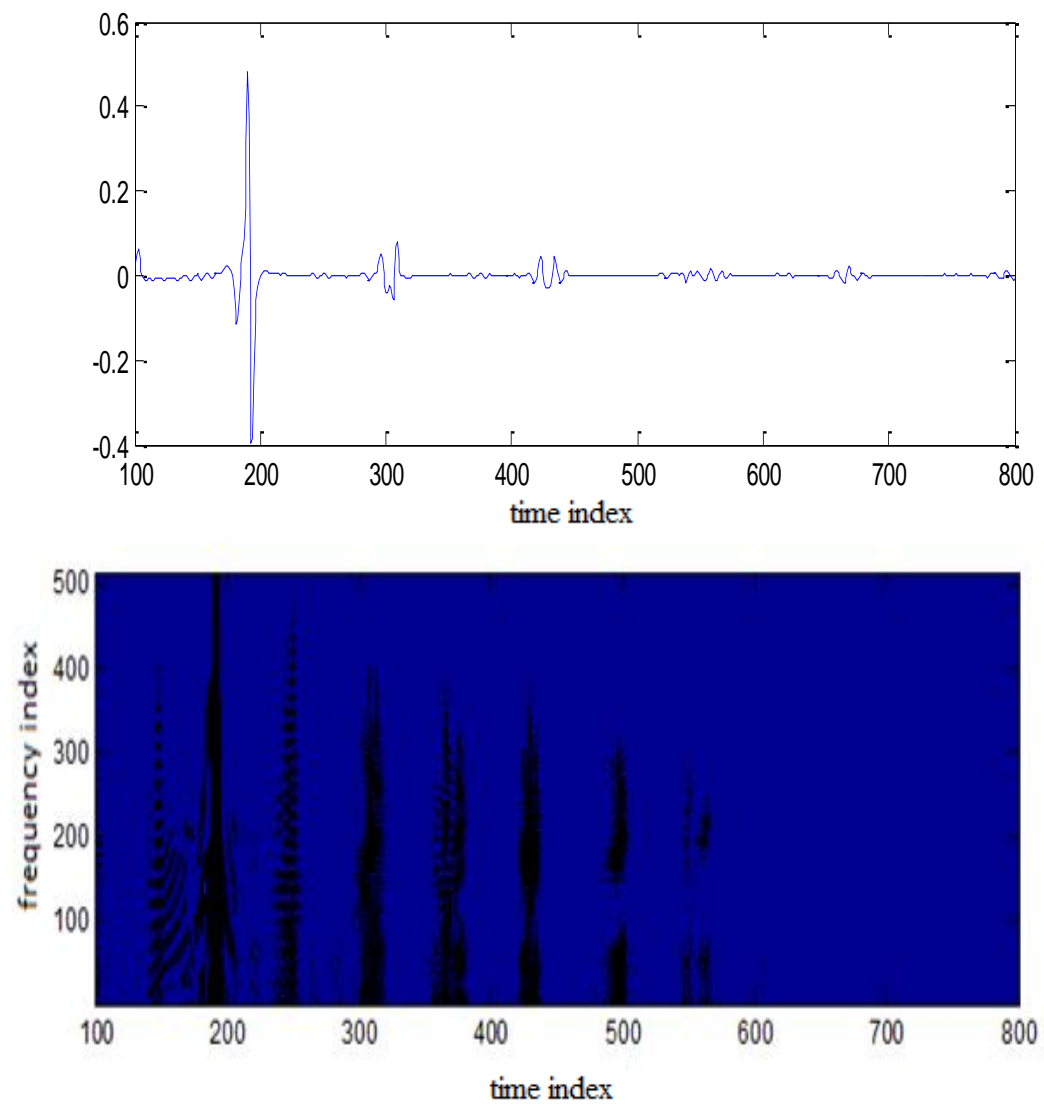

Figure 5.1 A sample signal and Wigner Distribution presentation of signal

33

5.2 Short Time Fourier Transform

The concepts of short-time Fourier analysis and synthesis are fundamental for describing any quasi-stationary (slowly time varying) signal such as speech. With the advent of the fast Fourier transform, as well as modem digital filtering techniques, implementations of signal processing systems based on the short-time Fourier transform have become practical and are used in many applications

where γ (t'-t) is the chosen window of analysis which is centered at t'=t and the superscript "*" denotes complex conjugation (Hlawatsch and Boudreaux-Bartels, 1992). As implied by this definition, the STFT of a signal may be interpreted as the local Fourier transform of the signal around the analysis time t.

$$STFT_x^{\gamma}(t,f) = \int_{t'} x(t')\gamma*(t'-t)e^{-j2\pi ft'}dt' \qquad (5.3)$$

5.3 Page Distribuiton

The Page distribution of a given time signal *x(t)* is defined as

$$PD_x(x,f) = \frac{d}{d_t}\left|\int_{-\infty}^{t} x(t')e^{-j2\pi ft'}dt'\right|^2 = 2\,\mathrm{Re}\left\{x^+(t)e^{j2\pi tf}\int_{-\infty}^{t} x(t')e^{-j2\pi ft'}dt'\right\} \qquad (5.4)$$

The Page Distribution is also an energetic, shift-invariant, quadratic TFR like the Wigner Distribution. Most of the desirable properties satisfied by the WD are also satisfied by the PD except for a few of them such as the property of having a finite frequency support (Hlawatsch and Boudreaux-Bartels, 1992).

6 APPLICATION AND RESULTS FOR TIME-FREQUENCY REPRESENTATIONS

In this part of the thesis, two location-independent strategies having "target-specific" and "signal-specific" optimum late-time intervals are designed by utilizing from time-frequency representations (TFRs) and corresponding energy distribution maps of the signals. To obtain the optimum late time starting points, proposed methods benefit from critical time-instants having maximum and especially mean power values (t_{max} and t_{mean}). Thus, even the distance of the target changes, these time instants almost equally shift, and the method finds the same optimum late-time interval. This situation provides being independent from distance of target. After having the optimum late-time intervals, one feature vector showing spectral energy densities of each target is extracted by using the same energy maps of TFRs over the selected optimum late-time intervals. In the test stage, a similar (test) vector of a test signal is acquired by using the same TFR/energy distribution and determined late-time intervals. Eventually, the classification is done relying on the highest correlation between test vector and feature vectors of targets. The offered strategies are realized with dielectric spheres at different locations.

6.1 Determination of Optimum Late Time Starts

Radar signals have been analyzed in either the time or the frequency domain. For analyzing and processing the datas coming from any radar system, generally Fourier transform is used. However, in radar systems generally time varying frequency values are observed for radar signals. But, Fourier transform analysis is not suitable for analyzing non-stationary signals.

Recently, while studying on transient scattering of targets, time-frequency representations has been used in the resonance region. For instance, the Wigner-Ville distribution of a sample scattered signal in Figure 6.1(a) is shown in Figure 6.1(b) and time-frequency distribution of x(t) signal is found by using the Wigner transform shown in previous equations.
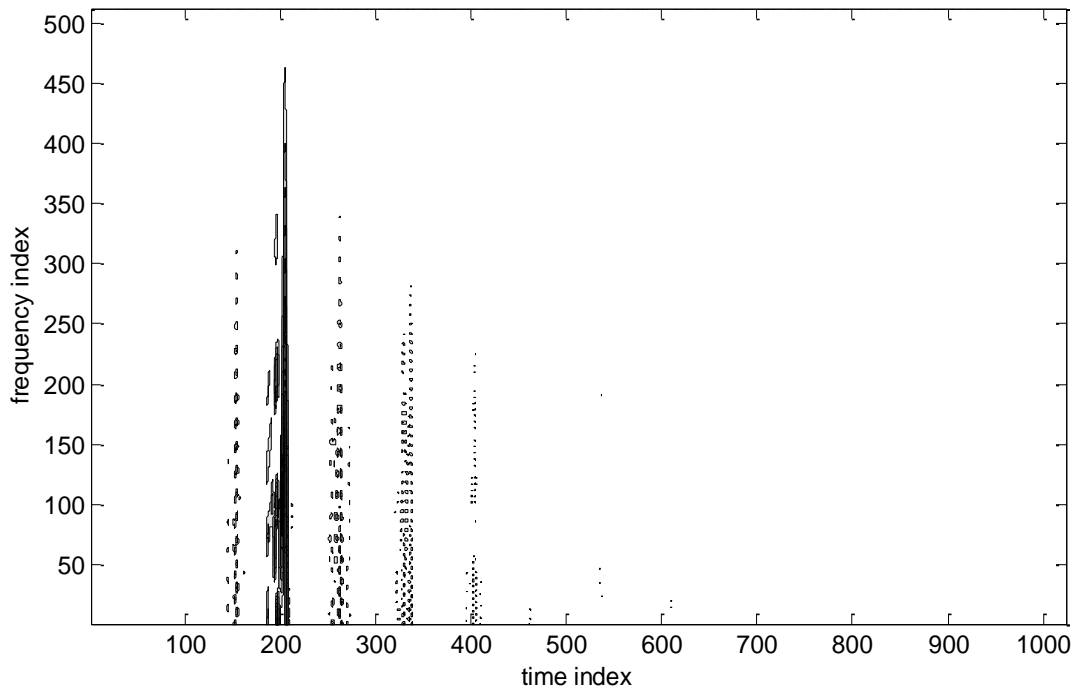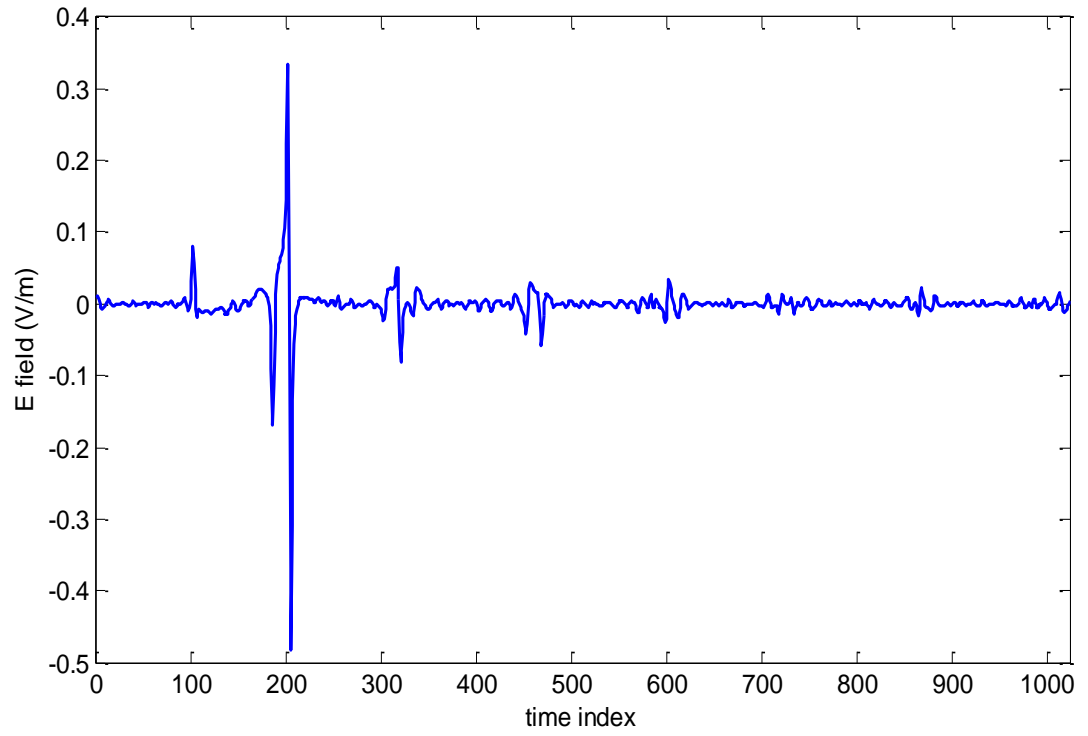
Figure 6.1 (a) A sample scattered signal (b) its Wigner-Ville distribution $\varepsilon_r=4$ $\theta=179°$

When (6.1) is applied all frequency values for each time index, instantaneous power is obtained and integrating all time values for each frequency gives the energy spectral density as in (6.2).

$$\int W_s(t,\omega)d\omega = |s(t)|^2 \tag{6.1}$$

$$\int W_s(t,\omega)dt = |S(\omega)|^2 \tag{6.2}$$

The first and most important step in the proposed strategies is to determine the optimum late-time start for each signal or target. For this purpose, a normalized instantaneous power curve along the time axis is obtained by first adding all values along the frequency axis in TFR for each time index and taking the square root with following equation;

$$\sqrt{\int W_s(t,\omega)d\omega} = |s(t)| \tag{6.3}$$

Then, the critical time instants corresponding to maximum and mean power values are found in the normalized curve. As an example, the normalized power curve for the distribution in Figure 6.1(a) is depicted in Fig. 6.2. As shown in the figure, time indices of 206 and 669 are t_{max} and t_{mean}, respectively.
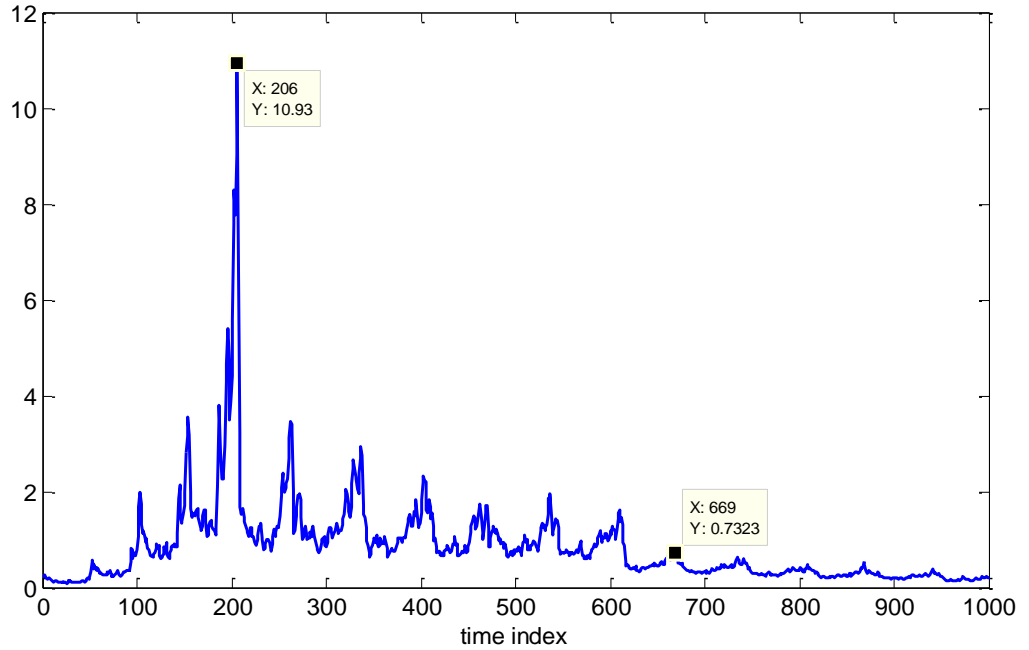
Figure 6.2 Normalized power curve for the scattered signal in Fig. 6.1(a)

In the thesis, t_{mean} is selected as time interval starting point for the "signal specific" method. (669th index in Fig 6.2) The reason behind this choice is that the effects of forced response and non-dominant poles are sufficiently suppressed until t_{mean} after which the power levels of the signal drop below the average, and the effects of dominant poles only remain after t_{mean}. However "target specific" method uses both t_{mean} and t_{max} by using the difference between them as (669-206=463 in Fig.). Independency from distances of the targets is an important issue and selection of time intervals/starting point in this way provides this necessity. Even the targets are closer to or further away the radar system, the difference between t_{max} and t_{mean} almost remains the same.

## 6.2   Extraction of Feature Vectors and Test Stage

In the feature extraction stage, belonging to aspect angles, moderate number of time-scattering signals is handled for each target. Afterwards, the critical t_{max} and t_{mean} time instants are found for each reference signal as described in previous section. In "signal specific" method, each reference signal determines its late-time start as its t_{mean} value. In "target specific" method, the differences of t_{max} and t_{mean} time instants at the reference signals of a target are calculated, and the highest difference value is kept for this target (let say 463). Then, the late-time start of each reference signal of the target is selected by adding this highest difference to t_{max} of each reference signal. For example, while late-time start is 206+463=669 for the reference signal in Figure 6.2, it can be 180+463=643 for another reference signal of the same target. This procedure is repeated for each target in the classifier. Although t_{max} is specific to the signal, because the added time difference is dependent on the target, the strategy is called as "target-specific".

After determination of late time starting points and intervals, a vector in the frequency axis showing spectral energy density of each frequency is acquired. This can be done by summing energy distribution values of TFRs along time axis over the selected late-time interval of the signal. This vector gives peaks nearly at the dominant pole frequencies that unique to target (SEM). These vectors also reduced into one by using PCA method. (Secmen M. 2011). Afterwards, this single vector is stored as feature vector and this step is repeated for each target.

Energy distribution is extracted for a test signal by using same TFRs in the classification stage. Then, t_{max} and t_{mean} time instants of the signal are found, and the late-time start/interval of the signal is determined. The late-time starts from t_{mean} and only one test vector is synthesized for test signal for the "signal specific" method. Then, comparison of this vector with all feature vectors of the targets is done one by one and test target is classified as the target having highest correlation coefficient. Firstly, t_{max} of test signal is calculated in the "target specific" method. Target specific method stores the highest time difference for the first target (for example 463) and this difference is added to t_{max} of test signal and late-time start is designated. Then, correlation coefficient between this vector and the feature of first target only is calculated. These all steps are repeated for the other targets to find the correlations and also second test vector is compared only with the feature vector of second target, and it continues in this way. The difference between "signal specific" and "target specific" methods is that in "target specific" method, there are test vectors as many as the number of the targets. However, each test vector is only compared with the corresponding feature vector. Finally, according to the highest correlation coefficient, classification is done among all calculated coefficients.

6.3   Simulation and Results

Lossless dielectric spheres are used to verify validity of suggested methods. Lossless dielectric spheres are geometrically simple targets but their scattering mechanisms are highly complex and challenging due to creeping (surface) waves and internal reflections/scatterings. In the thesis, making a fair comparison with the study (Turhan Sayan 2005), which depends on "classifier specific" late-time interval, test targets and corresponding parameters are handled the same with it. The problem geometry is given in Figure 6.3. Four targets are examined, and their radii and dielectric constants are used as a =10 cm and ε_r = 3, 4, 5 and 6 respectively. Different distances of targets for any aspect angles are selected to reduce dependency on location. Accordingly, the "r" value in Figure 6.3 (distance of the observation point) varies with target/aspect angle combination.
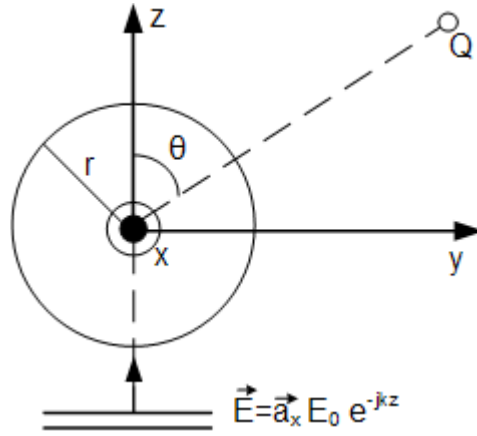
Figure 6.3 The dielectric sphere geometry used in application.

The scattered fields are generated by using classical Mie series in frequency domain with the frequency band of 0-19.2 GHz and 512 equally spaced frequency samples. The bistatic aspect angles are selected as θ= 5°, 15°, 30°, 45°, 60°, 75°, 90°, 105°, 120°, 135°, 150°, 165° and 179° for each target, and time domain scattered signals are synthesized by using IFFT and low pass Gaussian window. Consequently, a total of 13 ×4= 52 scattered signals for ε_r = 4 (Target 2) and θ =179°, are formed. Five aspect angles (θ = 5°, 45°, 90°, 135°, 179°) among all aspect angles are selected as reference aspect angles. The optimum late-time intervals are chosen as two successive time intervals with 64 time samples in order to be consistent with the study of (Turhan Sayan 2005). For example "signal specific" method and signal in Figure 6.4 is combined with Wigner Ville distribution, time intervals can be shown as (669-732) and (733-796). Then having summation along time axis over the selected late-time intervals, energy spectral density for each signal is extracted. The final frequency vector for distribution is shown in Figure 6.4 Here the first 512 frequency indices belong to energy spectral densities of the frequencies for the time interval of (669-732), and the second 512 frequency indices belong to energy spectral densities of the frequencies for the time interval of (733-796).
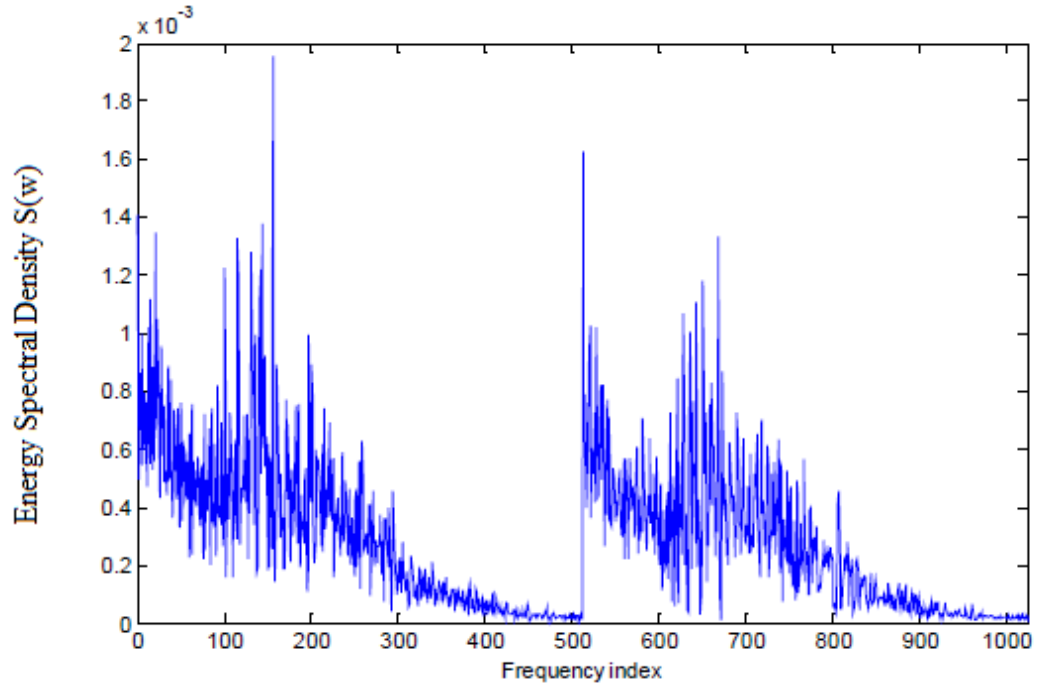
Figure 6.4 The processed frequency vector for the signal in Fig. 6a

For both methods of "target specific" and signal specific", optimum late-time intervals/start are extracted. In the classifier, the feature vector for each target is obtained with the method of PCA (dimension reduction technique) which is explained in previous sections. The feature vectors are demonstrated in Figure 6.5 and Figure 6.6 for the "signal specific" and "target specific" strategies, respectively. In the graphs, peak values represent the natural response frequencies.
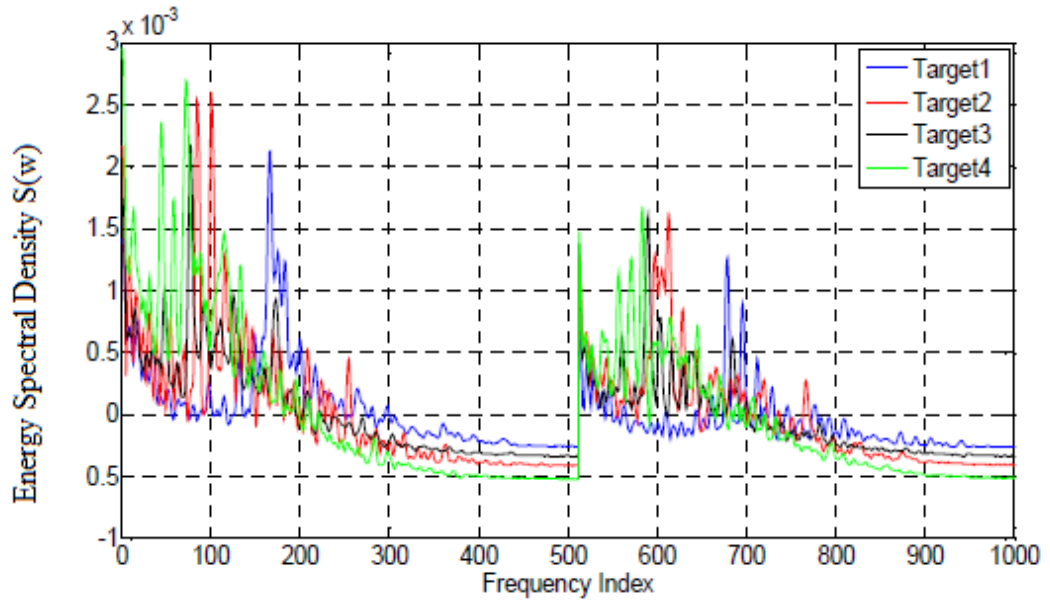
Figure 6.5 Feature vectors for "signal-specific" strategy.
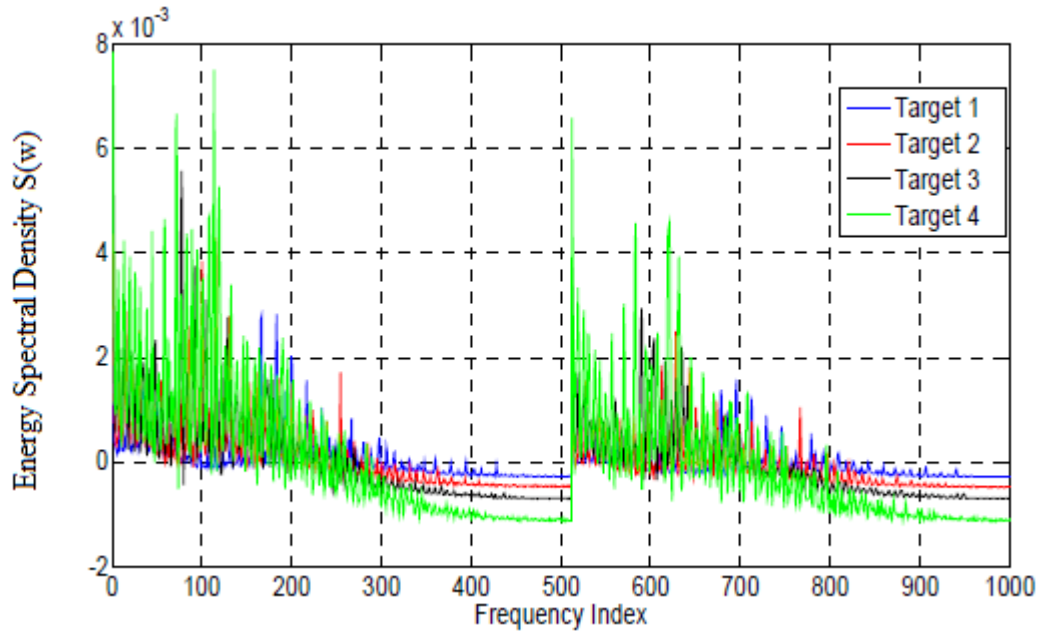
Figure 6.6 Feature vectors for "target-specific" strategy.

Noiseless situation is considered, and 52 scattered signals are tested. For both "target specific" method and "signal specific" method late-time intervals/starts are obtained and test frequency vectors are extracted. Same TFR methods are used for feature vector extraction stage but different correlation coefficient comparison procedure is done for each strategy. For example test frequency vector which is

42

generated by using "signal specific" method in Figure 6.5, and it is correlated with the feature vectors in Figure 6.4 one by one, for the signal in Figure 6.2. As the result of this comparison correlation coefficients are 0.5325, 0.7251, 0.5902, and 0.6010 for Targets 1, 2, 3, and 4, respectively. The with the high accuracy rates, test target is classified as Target 2 (the dielectric sphere with $\varepsilon_r = 4$). On the other hand, in the "target specific" method, four different test vectors are synthesized for the same test signal. Then, the first test frequency vector is only compared with the feature vector of Target 1, and the process continues until the last (fourth) test frequency vector is only compared with the feature vector of Target 4. The obtained correlation coefficients are obtained as 0.4949, 0.7742, 0.6505, and 0.5992 for the dielectric spheres with $\varepsilon_r = 3, 4, 5$ and 6, respectively.

In the following table performances and accuracy rates of some TFR methods are demonstrated such as Wigner-Ville (WV), Page (PG) distributions, their pseudo versions (SPWV and PPG) and STFT.

Table 6.1 The accuracy rates of the application with noise free signals for both methods and several TFRs (%)

Strategy	Time Frequency Representations				
	WV	PG	PWV	PPG	STFT
Signal Specific	100	78.85	84.62	86.54	88.46
Target Specific	100	67.31	92.31	84.61	92.31

It is easily understood from the table Wigner Ville distribution gves the higest accuraty percentages and also SPWV (pseudo Wigner) and STFT (short time Fourier transform) gives the higher than 88 percent for "target specific" method.

The performances of "target specific" and "signal specific" methods are also examined for noisy signals in the thesis. Methods and TFRs are compared with the study of (Turhan Sayan, 2005) for noisy signals, which also uses Wigner-Ville distribution and "classifier specific" late-time interval. However, the study of (Turhan Sayan, 2005) cannot be directly used for this application because of placing the targets at different distances to the receiver where the method in (Turhan Sayan,

2005) assumes that all targets are on the same distances. For this problem shifting time instants in absolute of all signals to a common time instant, can be a solution. After that the method of (Turhan Sayan, 2005) can be safely applied. But, it should be mentioned that offered methods in thesis do not need this kind of modification. Also noisy results for (Turhan Sayan, 2005) are also shown in the Table 4. The noisy signals are synthesized by contaminating noise-free signal with white Gaussian noise at the SNR levels of 25, 20, 15, 10, 7.5 and 5 dB. To reduce the dependency of the results to noise characteristic, 100 trials at each SNR level are realized. So, 52×100=5200 signals at each SNR level are totally used for testing purpose.

Table 6.2 The accuracy rates in percentage with noisy signals for both strategies of several TFRs and mentioned in (Turhan Sayan, 2005)

Strategy or Method	SNR (dB)						
	∞	25	20	15	10	7.5	5
Signal Specific (WV)	100	99	97.1	91.8	85.3	79.6	66
Target Specific (WV)	100	100	99.7	96	86	80.2	71
Signal Specific (STFT)	89	89	89.5	77.8	54	45.9	38
Signal Specific (SPWV)	79	78	78	76.9	73.8	71.1	69
Target Specific (STFT)	92	91	85.1	74.3	62.9	55.6	48
Target Specific (SPWV)	88	88	88.4	86.1	82.5	77.1	76
Classifier Specific (Turhan Sayan, 2005)	100	100	99.5	94	83.6	75.1	63

It is seen that from the table "target specific" method using Wigner Ville distribution gives the highest accuracy rates for SNR value higher then 7.5 dB. Suggested method gives the rates over 80 percent at the other SNR values and this can be regarded as sufficient performance for the classification. For the "signal specific" method Wigner Ville distribution with SPWV gives the over 75 percent accuracy rate even in 5 dB. "Signal specific" method gives the better results at low

SNR values however it gives the low rates at high dB values compared to "target specific" and the study (Turhan Sayan, 2005). On the other hand "target specific" method and (Turhan Sayan, 2005) are compared with each other they have similar values at high noisy levels, but at low SNR values decrease become sharper. In STFT method accuracy rates fall down under un-expected percentages so STFT method is not a sufficient method to apply. Here the graphical representation of the Table 6.1 is given and accuracy rates versus SNR values are shown.
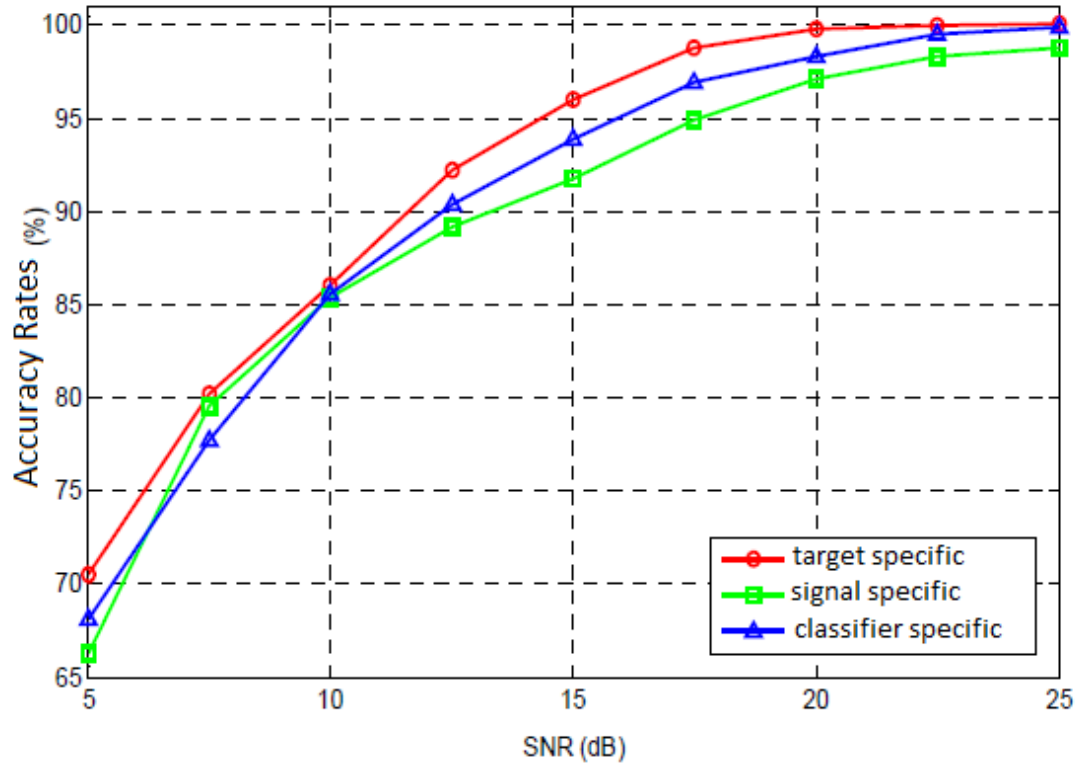
Figure 6.7 Graphical shown of values in suggested methods (Table 6.1) and (Turhan Sayan, 2007)

As seen from the Figure 6.7, "target specific" method gives the best performance, even at SNR=5 dB value, this suggested method gives the rate over 70 percent. "Signal specific" method gives good performances only at low SNR values but it is in-sufficient at high SNR values. The reason for this situation is that t_{mean} values are found far away from desired at high SNR values and at low SNR values t_{mean} values can be taken more reasonable region. Especially the "target-specific" method pretends this undesired situation and increaes the accuracy percentages. The

45

"classifier specific" method presented in the study of (Turhan Sayan, 2005) also gives enough performances. However these important points should not be ignored. In this application, to realize a fair comparison while obtaning scattered signals in the study of (Turhan Sayan, 2005), it is assumed that all targets are in the same position. This hypothesis can be partially applied for real-time applications but the location of test targets will be different from reference location. It means that 641th index will be coincided with more late or more early time interval. Thus, especially if the targets are in different locations, accuracy rates will fall down. On the other hand, suggested "signal-specific" and "target-specific" methods select t_{max} and t_{mean} values as reference so it does not effect the performance of these methods.

7   CONCLUSION AND FUTURE WORK

7.1   Conclusion

In the thesis target recognition with high resolution techniques and time frequency representations are explained for different strategies.

For the first study in the chapter 3, firstly feature vectors are extracted that sufficiently aspect independent for each target. Then, using the convenient time intervals of reference signals, ESPRIT spectrum vectors are obtained. PCA dimension reduction technique is applied to ESPRIT vectors of each target, which are as many as the number of reference aspect angles for reducing to the a single ESPRIT feature vector.

In the test stage, the calculated test ESPRIT spectrum vectors are compared with feature vectors of the known targets and classification is done due to highest correlation coefficient. The suggested method in this chapter has been successfully applied to a set of small-scale airplane targets whose dimensions are slightly different from one to another. In noise-free situation offered method gives the 100 percent accuracy rate. This rate solely drops to about 88 percent at a severely noisy level of SNR = -5 dB. It is also understood that PCA technique gives better performances compared to other dimension reduction techniques.

In the other study presented in chapter 5, in offered both "signal specific" and "target specific" methods, it is utilized from a time-frequency representation (mainly in Wigner-Ville in this study) in the determination of optimum late time commence instant/late-time interval and extraction of feature vectors. In suggested methods, the determined late-time intervals are highly insensitive to distance of the target, and the extracted feature vectors include aspect-independent frequency information which are unique to target. Both "signal specific" and "target specific" methods are simulated with dielectric spheres which are located at different positions and obtained result are compared for the several different TFRs and similar methods in the literature. According to simulation and comparison results, combination of Wigner Ville method and "target specific" strategy give best performances among all similar methods.

7.2   Future Work

The future work will be about usage of wavelets for target recognition and classification with time-frequency representation techniques (TFR's). Results of wavelet applications will be examined and comparisons with other methods in the literature will be obtained.

REFERENCES

Baum C. E., 1976, The Singularity Expansion Method. Transient Electromagnetic Fields. Editör: Felsen, L. B. Berlin: Springer-Verlag.

Baum C. E., Rothwell, E. J., Chen, K.-M., and Nyquist, D. P., 1991, The singularity expansion method and its application to target identification, Proc. IEEE, 79(10), 1481-1492.

C. A. Balanis, 2005, Antenna Theory-Analysis and Design, 3rd ed., John Wiley & Sons Inc., Hoboken, New Jersey.

C.I. Chuang, D. P. Nyquist, K.M. Chen, and B. C. Drachman, 1985 "Singularity expansion method formulation for impulse response of a perfectly conducting thick cylinder," Radio Science, vol. 20, no. 5, pp. 1025-1030.

Chen W. C., Shuley N. V. Z., 2008, Resonance based target identification using principal component analysis, IEEE Asia-Pacific Microwave Conference (APMC), Macau, China.

Chen, W. C., Shuley N. V. Z., 2014, Robust Target Identification Using a Modified Generalized Likelihood Ratio Test," IEEE Trans. Antennas and Propagation, 62(1): 264-273.

Lee, K. C., Ou, J. S., and Fang, M. C., 2008, Application of SVD noise-reduction technique to PCA based radar target recognition, Progress in Electromagnetics Research (PIER), 81, 447-459.

Lui, H.-S., Aldhubaib, F., Shuley, N. V. Z., and Hui, H.-T., 2009, Subsurface target recognition based on transient electromagnetic scattering, IEEE Trans. on Antennas and Propagation, 57(10), 3398-3401.

Lui, H.-S., Shuley, N. V. Z., and Rakic, A. D., 2010, A Novel, Fast, Approximate Target Detection Technique for Metallic Target Below a Frequency Dependant Lossy Halfspace, IEEE Trans. Antennas and Prop., 58(5):1699-1710.

Lui, H.-S., Shuley N. V. Z., 2010, Performance evaluation of subsurface target recognition based on ultrawideband short-pulse excitation, IEEE Antennas and Propagation Society International Symposium, Toronto, Canada.

Harmer, S. W., Andrews, D. A., Rezgui, N. D., and Bowring, N. J., 2010a, Detection of handguns by their complex natural resonant frequencies, IET Microw. Antennas Propag. 4(9), 1182-1190.

Harmer, S. W., Cole, S. E., Bowring, N. J., Rezgui, N. D., and Andrews, D., 2010b, On body concealed weapon detection using a phased antenna array, Progress in Electromagnetics Research (PIER), 124, 187-210.

Hlawatsch, F., Boudreaux-Bartels, G. F., 1992, "Linear and Quadratic Time-Frequency Signal Representations," IEEE Signal Processing Mag., 9(2): 21-67.

Jackson J. E., 2003, A User's Guide to Principal Components, John Wiley & Sons Inc., Hoboken, New Jersey.

Jackson, J. E., 2003, A User's Guide to Principal Components, John Wiley, Hoboken, N. J.

K. C. Lee, J. S. Ou, and M. C. Fang, 2008, Application of SVD noise reduction technique to PCA based radar target recognition, Progress In Electromagnetics Research, vol.81, pp. 447-459.

Kim, K.T., I.S. Choi, and H.T. Kim, 2000, Efficient radar target classification using adaptive joint time-frequency processing, IEEE Trans. Antennas Propag., 48(12), 1789–1801, doi:10.1109/8.901267.

Kim, K.T., I.S. Choi, and H.T. Kim, 2002, Efficient radar target recognition using the MUSIC algorithm and invariant features, IEEE Trans. Antennas Propag., 50(3), 325–337, doi:10.1109/8.999623.

Kitamura, M., J.I. Takada, and K. Araki, 1999, A model order estimation in the Matrix Pencil method for the transient response of a microwave circuit discontinuity, IEICE Trans. Electron., 82(11), 2081–2086.

Makal, S., Durak, L., and Kızılay, A., 2008a, "Dalgacık Dönüşümü ve ROC Analizi Yardımıyla Silindirik Hedeflerin Sınıflandırılması", IEEE Sinyal İşleme ve İletişim Uygulamaları Kurultayı (SİU), Aydın, Turkey.

Makal, S., Kizilay, A., and Durak, L., 2008b, "On the target classification through waveletcompressed scattered ultrawide-band electric field data and ROC analysis", Progress in Electromagnetics Research (PIER), 82, 419-431.

Rothwell, E. J., Chen, K.-M., Nyquist, D. P., Ilavarasan, P., Ross, J. E., Bebermeyer, R., and Li, Q., 1994, A general E-pulse scheme arising from the dual early-time/late-time behavior of radar scatterers, IEEE Trans. on Antennas and Propagation, 42(9), 1336-1341.

Secmen M., 2008, A novel music algorithm based electromagnetic target recognition method in resonance region for the classification of single and multiple targets, (Ph. D. Thesis), Middle East Technical University Engineering Faculty.

Secmen M., Turhan-Sayan G., 2009, Radar target classification method with reduced aspect dependency and improved noise performance using multiple signal classification algorithm, IET Radar, Sonar and Navigation, 3(6), 583-595.

Secmen M., 2011a, The application of fusion of multiple aspect scattered data to PMUSIC vector based electromagnetic target identification, IEEE Antennas and Propagation Society International Symposium, Spokane, WA, ABD.

Secmen M., 2011b, Radar target classification method with high accuracy and decision speed performance using MUSIC spectrum vectors and PCA projection, Radio Science, 46(RS5015), 1-9.

Secmen M., 2012, Extraction of electromagnetic target poles from multiple scattered fields with damped Min-norm method, Int. Journal of Electronics and Communication (AEÜ), vol. 66, no. 10, pp. 860-863, 2012.

Skolnik M. I., 2001, Introduction to radar systems, Mc Graw-Hill, 3rd ed., New York.

Stoica P. and Moses R., 2005, Spectral Analysis of Signals, Pearson, Upper Saddle River, New Jersey.

Turhan-Sayan, G., 2005, Real time electromagnetic target classification using a novel feature extraction technique with PCA-based fusion, IEEE Trans. Antennas Propag., 53(2), 766–776.

Vasalos A., Ryu H. G., Vasalos I. and Fotinea S.-E., 2011, Fast concealed weapon detection via LTR analysis," IEEE Radar Conference, pp. 979- 984.

Zhang L., Hao, Y. Parini, C. G., 2007, Natural resonant frequency extraction for concealed weapon detection at millimetre wave frequencies, The Second European Conference on Antennas and Propagation (EUCAP), Edinburgh, Scotland.

Zhang L., 2011, Millimetre Wave Imaging for Concealed Target Detection, (Ph. D. Thesis), University of London, London, United Kingdom.

APPENDIX A

SAMPLE CODE OF CLASSIFICATION OF A SAMPLE TARGET (PLANE 1) WITH HIGH RESOLUTION TECHNIQUES

```matlab
clear
close all
N=65;
m=33;
L=6;
f= 0:1/512:0.5;
signal = 37;
plane_1 = [3 10 19 28 35];
plane_2 = plane_1 + signal;
plane_3 = plane_2 + signal;
plane_4 = plane_3 + signal;
load xnorm_eski.mat
xnorm(3,:);
xnorm(10,:);
xnorm(19,:);
xnorm(28,:);
xnorm(35,:);
hh = hankel(xnorm(plane_1(1),:));
R=hh(1:33,1:33);
 [U,D,V] = svd(R);
I=eye(m-1);
O=zeros(m-1,1);
I1=[I,O];
I2=[O,I];
S1=I1*U(:,1:L);
S2=I2*U(:,1:L);
Psi=inv(S1'*S1)*S1'*S2;
zi=eig(Psi);
a=poly(zi);
for c=1:257
 e_f(:,c)=exp(-j*2*pi*f(c)*(0:L)).';
end
P_f_1=1./abs(a*e_f).^2;
S_1(1,:) = P_f_1./norm(P_f_1);
xlabel('Frequnecy(Hz)');
ylabel('Amplitude');
grid
hh = hankel(xnorm(plane_1(2),:));
R=hh(1:33,1:33);
[U,D,V] = svd(R);
```

```matlab
I=eye(m-1);
O=zeros(m-1,1);
I1=[I,O];
I2=[O,I];
S1=I1*U(:,1:L);
S2=I2*U(:,1:L);
Psi=inv(S1'*S1)*S1'*S2;
zi=eig(Psi);
a=poly(zi);
 for c=1:257
 e_f(:,c)=exp(-j*2*pi*f(c)*(0:L)).';
end
P_f_2=1./abs(a*e_f).^2;
S_1(2,:) = P_f_2./norm(P_f_2);
xlabel('Frequnecy(Hz)');
ylabel('Amplitude');
grid
hh = hankel(xnorm(plane_1(3),:));
R=hh(1:33,1:33);
 [U,D,V] = svd(R);
I=eye(m-1);
O=zeros(m-1,1);
I1=[I,O];
I2=[O,I];
S1=I1*U(:,1:L);
S2=I2*U(:,1:L);
Psi=inv(S1'*S1)*S1'*S2;
zi=eig(Psi);
a=poly(zi);
for c=1:257
 e_f(:,c)=exp(-j*2*pi*f(c)*(0:L)).';
end
P_f_3=1./abs(a*e_f).^2;
S_1(3,:) = P_f_3./norm(P_f_3);
xlabel('Frequnecy(Hz)');
ylabel('Amplitude');
grid
hh = hankel(xnorm(plane_1(4),:));
R=hh(1:33,1:33);
 [U,D,V] = svd(R);
I=eye(m-1);
O=zeros(m-1,1);
I1=[I,O];
I2=[O,I];
S1=I1*U(:,1:L);
S2=I2*U(:,1:L);
Psi=inv(S1'*S1)*S1'*S2;
```

```matlab
zi=eig(Psi);
a=poly(zi);
for c=1:257
 e_f(:,c)=exp(-j*2*pi*f(c)*(0:L)).';
 end
P_f_4=1./abs(a*e_f).^2;
S_1(4,:) = P_f_4./norm(P_f_4);
xlabel('Frequnecy(Hz)');
ylabel('Amplitude');
grid
hh = hankel(xnorm(plane_1(5),:));
R=hh(1:33,1:33);
 [U,D,V] = svd(R);
I=eye(m-1);
O=zeros(m-1,1);
I1=[I,O];
I2=[O,I];
S1=I1*U(:,1:L);
S2=I2*U(:,1:L);
Psi=inv(S1'*S1)*S1'*S2;
zi=eig(Psi);
a=poly(zi);
for c=1:257
 e_f(:,c)=exp(-j*2*pi*f(c)*(0:L)).';
end
P_f_5=1./abs(a*e_f).^2;
S_1(5,:) = P_f_5./norm(P_f_5);
xlabel('Frequnecy(Hz)');
ylabel('Amplitude');
grid
PLANE1 = sum(S_1);
[U,D,V]=svd(cov(S_1(1:5,:)'));
   D1=diag(D);
   absurd=mean(S_1(1:5,:),2)*ones(1,257);
   as=S_1(1:5,:)-absurd;
   pc=V'*as;
yer1=D1(1)*pc(1,:)/sum(D1)+D1(2)*pc(2,:)/sum(D1)+D1(3)*pc(3,:)/sum(D1);
   yer1=-yer1./norm(yer1);
   save yer1.mat yer1
plot(f,yer1,'m');
hold
plot(f,PLANE1/norm(PLANE1)-mean(PLANE1/norm(PLANE1)));
plot(f,sum(as)/norm(sum(as)),'k');
xlabel('Frequnecy(Hz)');
ylabel('Amplitude');
grid
```

%% TEST STAGE %%

```
clear
N=65;
m=33;
L=6;
f= 0:1/512:0.5;
load yer1.mat
load yer2.mat
load yer3.mat
load yer4.mat
load xnorm_eski.mat
PLANE1_L4=yer1;
PLANE2_L4=yer2;
PLANE3_L4=yer3;
PLANE4_L4=yer4;
dogru_sayisi = 0;
tic
for iter=1:1
   for i = 1:148;
      clear z R y1
      noise=noisecg(length(xnorm(i,:)));
      realnoise=real(noise);
      realnoise=realnoise-mean(realnoise);
      y1(:,1)=sigmerge(xnorm(i,:)',realnoise,1000);
      z=mean(y1,2);
      hh = hankel(z);
      R=hh(1:33,1:33);
      [U,D,V] = svd(R);
      I=eye(m-1);
      O=zeros(m-1,1);
      I1=[I,O];
      I2=[O,I];
      S1=I1*U(:,1:L);
      S2=I2*U(:,1:L);
      Psi=inv(S1'*S1)*S1'*S2;
      zi=eig(Psi);
      a=poly(zi);
      for c=1:257
         e_f(:,c)=exp(-j*2*pi*f(c)*(0:L)).';
      end
      t = 0:10:100;
      P_f=1./abs(a*e_f).^2;
      plane_n = P_f./norm(P_f);
      plot(((1024*f)/0.5),plane_n);
      variable1 = corrcoef(plane_n,PLANE1_L4);
```

```matlab
        uyum1 = variable1 (1,2);
        variable2 = corrcoef(plane_n,PLANE2_L4);
        uyum2 = variable2 (1,2);
        variable3 = corrcoef(plane_n,PLANE3_L4);
        uyum3 = variable3 (1,2);
         variable4 = corrcoef(plane_n,PLANE4_L4);
        uyum4 = variable4 (1,2);
        uyumlar(i,:)=[uyum1 uyum2 uyum3 uyum4];
        [maximumlar,index]=max(uyumlar(i,:));
        ucak(i)=index;
    end
    for i=1:37
        if ucak(i) == 1
            dogru_sayisi = dogru_sayisi+1;
        end
    end
    for i=38:74
        if ucak(i) == 2
            dogru_sayisi = dogru_sayisi+1;
         end
    end
    for i=75:111
        if ucak(i) == 3
            dogru_sayisi = dogru_sayisi+1;
        end
    end
    for i=112:148
        if ucak(i) == 4
            dogru_sayisi = dogru_sayisi+1;
        end
    end
end
toc
yuzde_dogruluk = dogru_sayisi*100/(148*iter)
```

APPENDIX B

SAMPLE CODE FOR "SIGNAL SPECIFIC" METHOD

```matlab
clear all
close all
warning('off','MATLAB:dispatcher:InexactCaseMatch')
% 52 different signals are applied for the method
notgt=4;
no_angle=13;
tgtltd = notgt*no_angle;
  t_reference_angle =[f1; f4; f7; f10; f13; f14; f17; f20; f23; f26;
   f27; f30; f33; f36 ;f39 ;f40 ;f43 ;f46 ;f49 ;f52];
    for jj=1:size(t_reference_angle,1)
      y=t_reference_angle(jj,:);
      wi=real(tfrwv(y.'));
      TFRp=(abs(wi)+wi)/2;
      wigner(1:512,:)=TFRp(1:512,:);
      wig_column = sqrt(sum(wigner));
      [a,max_energy_index] = max(wig_column);
      max11(jj) = max_energy_index;
       [c,d]=find((wig_column(max_energy_index:end-
128)>0.85*mean(wig_column))        &        (wig_column(max_energy_index:end-
128)<1.15*mean(wig_column)));
      max22(jj)=d(end)+max_energy_index-1;
            temp1 = wigner(:,max22(jj):max22(jj)+63);
            temp2 = wigner(:,max22(jj)+64:max22(jj)+127);
        late1 = sum(temp1')/64;
        late2 = sum(temp2')/64;
        test_vector(:,jj) = [late1 late2];
    end
   for i = 1:4
        X = test_vector(:,((i-1)*5 + 1):(i*5));
        [PC, SCORE, LATENT, TSQUARE] = PRINCOMP(X);
        lambda1(:,i) = LATENT;
        PCA(:,i) = SCORE(:,1);
   end
   fark = max(max22-max11);
   for q =50:5:50
      yanlis = 0;
      dogru = 0;
      for deneme = 1:1
         for jj = 1:tgtltd

            temp1 = 0; temp2 = 0; y1=0;
```

```
            y = ALL(jj,:);
            noise = noisecg(length(y)); realnoise = real(noise);
            realnoise = realnoise-mean(realnoise);
            y1 = sigmerge(y',realnoise,q);
            wi = real(tfrwv(y1));
            TFRp = (abs(wi)+wi)/2;
            wigner(1:512,:) = TFRp(1:512,:);
            wig_column = sqrt(sum(wigner));
            [a,max_energy_index] = max(wig_column);
            max1(jj) = max_energy_index;
[c,d]=find((wig_column(max_energy_index:end-128)>0.85*mean(wig_column))    &
(wig_column(max_energy_index:end-128)<1.15*mean(wig_column)));
            max2(jj)=d(end)+max_energy_index-1;
            temp1 = wigner(:,max2(jj):max2(jj)+63);
            temp2 = wigner(:,max2(jj)+64:max2(jj)+127);
            late1 = sum(temp1')/64;
            late2 = sum(temp2')/64;
            test_vector1(:,jj) = [late1 late2];
          end
          for kf1 = 1:tgtltd
            for t = 1:notgt
               dummy3 = PCA(:,t);
               res = corrcoef(test_vector1(:,kf1),dummy3);
               result(t) = res(1,2);
            end
            sumresult(kf1,:) = result;
          end;
          for trg = 1:notgt
            alim = (trg-1)*no_angle+1;
            ulim = trg*no_angle;

            for rr = alim:ulim
               [ymax,II] = max(sumresult(rr,:));
               if II ~= trg
                  yanlis = yanlis+1;
               end
               if II == trg
                  dogru = dogru+1;
               end
            end
          end
       end
       dogru
       yanlis
       RD = 100*dogru/(tgtltd*deneme)
     end
     toc
```

APPENDIX C

SAMPLE CODE FOR "TARGET SPECIFIC" METHOD

```
clear all
close all
warning('off','MATLAB:dispatcher:InexactCaseMatch')
% 52 sifferent signals are applied for the method
notgt = 4;
no_angle = 13;
tgtltd = notgt*no_angle;
t_reference_angle = [f1; f4; f7; f10; f13; f14; f17; f20; f23; f26;
            f27; f30; f33; f36 ;f39 ;f40 ;f43 ;f46 ;f49 ;f52];
 for jj = 1:5
   y = t_reference_angle(jj,:);
   wi = real(tfrwv(y.'));
   TFRp = (abs(wi)+wi)/2;
   wigner(1:512,:)=TFRp(1:512,:);
   wig_column = sqrt(sum((wigner)));
   [a,max_energy_index] = max(wig_column);
   max1(jj) = max_energy_index;
   [b,half_max_energy_index]    =    min(abs(wig_column(max_energy_index:end)-
mean(wig_column)));
   [c,d]=find((wig_column(max_energy_index:end-128)>0.8*mean(wig_column))  &
(wig_column(max_energy_index:end-128)<1.2*mean(wig_column)));
   max2(jj)=d(end)+max_energy_index-1;
end
for z = 6:10
   y2 = t_reference_angle(z,:);
   wi = real(tfrwv(y2.'));
   TFRp = (abs(wi)+wi)/2;
   wigner(1:512,:) = TFRp(1:512,:);
   wig_column = sqrt(sum((wigner)));
   [a,max_energy_index] = max(wig_column);
   max3(z-5) = max_energy_index;
   [c,d]=find((wig_column(max_energy_index:end-128)>0.8*mean(wig_column))  &
(wig_column(max_energy_index:end-128)<1.2*mean(wig_column)));
   max4(z-5)=d(end)+max_energy_index-1;
end
for t = 11:15
   y3 = t_reference_angle(t,:);
   wi = real(tfrwv(y3.'));
   TFRp = (abs(wi)+wi)/2;
   wigner(1:512,:) = TFRp(1:512,:);
   wig_column = sqrt(sum((wigner)));
```

```
    [a,max_energy_index] = max(wig_column);
    max5(t-10) = max_energy_index;
    [c,d]=find((wig_column(max_energy_index:end-128)>0.8*mean(wig_column))  &
(wig_column(max_energy_index:end-128)<1.2*mean(wig_column)));
    max6(t-10)=d(end)+max_energy_index-1;
end
for r = 16:20
    y4 = t_reference_angle(r,:);
    wi = real(tfrwv(y4.'));
    TFRp = (abs(wi)+wi)/2;
    wigner(1:512,:)=TFRp(1:512,:);
    wig_column = sqrt(sum((wigner)));
    [a,max_energy_index] = max(wig_column);
    max7(r-15) = max_energy_index;
    [c,d]=find((wig_column(max_energy_index:end-128)>0.95*mean(wig_column))
& (wig_column(max_energy_index:end-128)<1.05*mean(wig_column)));
    max8(r-15)=d(end)+max_energy_index-1;
end
max_total = [max2-max1; max4-max3; max6-max5; max8-max7]';
avg_max = round(max(max_total))
for jj = 1:5
    temp1 = 0;
    temp2 = 0;
    y = t_reference_angle(jj,:);
    wi = real(tfrwv(y.'));
    TFRp = (abs(wi)+wi)/2;
    wigner(1:512,:)=TFRp(1:512,:);
    wig_column = sqrt(sum((wigner)));
    [a,max_energy_index] = max(wig_column);
   avg_max1(1)=avg_max(1)+max_energy_index;
    temp1 = wigner(:,avg_max1(1):avg_max1(1)+63);
    temp2 = wigner(:,avg_max1(1)+64:avg_max1(1)+127);
    late1 = sum(temp1')/64;
    late2 = sum(temp2')/64;
    ref_vector1(:,jj) = [late1 late2];
end
for z = 6:10
    temp3 = 0;
    temp4 = 0;
    y2 = t_reference_angle(z,:);
    wi = real(tfrwv(y2.'));
    TFRp = (abs(wi)+wi)/2;
    wigner(1:512,:)=TFRp(1:512,:);
     wig_column = sqrt(sum((wigner)));
    [a,max_energy_index] = max(wig_column);
   avg_max1(2)=avg_max(2)+max_energy_index;
    temp3 = wigner(:,avg_max1(2):avg_max1(2)+63);
```

```
    temp4 = wigner(:,avg_max1(2)+64:avg_max1(2)+127);
    late3 = sum(temp3')/64;
    late4 = sum(temp4')/64;
    ref_vector2(:,z-5) = [late3 late4];
end
for t = 11:15
    temp5 = 0;
    temp6 = 0;
    y3 = t_reference_angle(t,:);
    wi = real(tfrwv(y3.'));
    TFRp = (abs(wi)+wi)/2;
    wigner(1:512,:)=TFRp(1:512,:);
    wig_column = sqrt(sum((wigner)));
    [a,max_energy_index] = max(wig_column);
    avg_max1(3)=avg_max(3)+max_energy_index;
    temp5 = wigner(:,avg_max1(3):avg_max1(3)+63);
    temp6 = wigner(:,avg_max1(3)+64:avg_max1(3)+127);
    late5 = sum(temp5')/64;
    late6 = sum(temp6')/64;
    ref_vector3(:,t-10) = [late5 late6];
end
for r = 16:20
    temp7 = 0;
    temp8 = 0;
    y4 = t_reference_angle(r,:);
    wi = real(tfrwv(y4.'));
    TFRp = (abs(wi)+wi)/2;
    wigner(1:512,:)=TFRp(1:512,:);
    wig_column = sqrt(sum((wigner)));
    [a,max_energy_index] = max(wig_column);
    avg_max1(4)=avg_max(4)+max_energy_index;
    temp7 = wigner(:,avg_max1(4):avg_max1(4)+63);
    temp8 = wigner(:,avg_max1(4)+64:avg_max1(4)+127);
    late7 = sum(temp7')/64;
    late8 = sum(temp8')/64;
    ref_vector4(:,r-15) = [late7 late8];
end
for iii = 1
    X_1 = ref_vector1(:,((iii-1)*5 + 1):(iii*5));
    [PC, SCORE, LATENT, TSQUARE] = PRINCOMP(X_1);
    lambda1(:,iii) = LATENT;
    PCA1(:,iii) = SCORE(:,1);
    X_2 = ref_vector2(:,((iii-1)*5 + 1):(iii*5));
    [PC, SCORE, LATENT, TSQUARE] = PRINCOMP(X_2);
    lambda1(:,iii) = LATENT;
    PCA2(:,iii) = SCORE(:,1);
    X_3 = ref_vector3(:,((iii-1)*5 + 1):(iii*5));
```

```matlab
    [PC, SCORE, LATENT, TSQUARE] = PRINCOMP(X_3);
    lambda1(:,iii) = LATENT;
    PCA3(:,iii) = SCORE(:,1);
    X_4 = ref_vector4(:,((iii-1)*5 + 1):(iii*5));
    [PC, SCORE, LATENT, TSQUARE] = PRINCOMP(X_4);
    lambda1(:,iii) = LATENT;
    PCA4(:,iii) = SCORE(:,1);
end
tic
    for q = 50:5:50
        temp1=0; temp2=0; temp3=0; temp4=0;
        temp5=0; temp6=0; temp7=0; temp8=0;
        yanlis = 0;
        dogru = 0;
        for deneme = 1:1
            for jj = 1:tgtltd
                y2=ALL(jj,:);
                wi=real(tfrwv(y2'));
                TFRp = (abs(wi)+wi)/2;
                wigner(1:512,:) = TFRp(1:512,:);
                wig_column = sqrt(sum((wigner)));
    [a,max_energy_index] = max(wig_column);
  avg_max2(1)=avg_max(1)+max_energy_index;
  avg_max2(2)=avg_max(2)+max_energy_index;
  avg_max2(3)=avg_max(3)+max_energy_index;
  avg_max2(4)=avg_max(4)+max_energy_index;
   temp1 = wigner(:,avg_max2(1):avg_max2(1)+63);
   temp2 = wigner(:,avg_max2(1)+64:avg_max2(1)+127);
            late1 = sum(temp1')/64;
            late2 = sum(temp2')/64;
            test_vector1(:,jj) = [late1 late2];
            temp3 = wigner(:,avg_max2(2):avg_max2(2)+63);
            temp4 = wigner(:,avg_max2(2)+64:avg_max2(2)+127);
            late3 = sum(temp3')/64;
            late4 = sum(temp4')/64;
            test_vector2(:,jj) = [late3 late4];
            temp5 = wigner(:,avg_max2(3):avg_max2(3)+63);
            temp6 = wigner(:,avg_max2(3)+64:avg_max2(3)+127);
            late5 = sum(temp5')/64;
            late6 = sum(temp6')/64;
            test_vector3(:,jj) = [late5 late6];
            temp7 = wigner(:,avg_max2(4):avg_max2(4)+63);
            temp8 = wigner(:,avg_max2(4)+64:avg_max2(4)+127);
            late7 = sum(temp7')/64;
            late8 = sum(temp8')/64;
            test_vector4(:,jj) = [late7 late8];
          end
```

```matlab
        for kf1 = 1:tgtltd
                res= corrcoef(test_vector1(:,kf1),PCA1);
                result(kf1,1) = res(1,2);
                res1= corrcoef(test_vector2(:,kf1),PCA2);
                result(kf1,2) = res1(1,2);
                res2= corrcoef(test_vector3(:,kf1),PCA3);
                result(kf1,3) = res2(1,2);
                res3= corrcoef(test_vector4(:,kf1),PCA4);
                result(kf1,4) = res3(1,2);
            end;
            sumresult= result;
            for trg = 1:notgt
                alim = (trg-1)*no_angle+1;
                ulim = trg*no_angle;
                for rr = alim:ulim
                    [ymax,II] = max(sumresult(rr,:));
                    if II ~= trg
                        yanlis = yanlis+1;
                    end
                    if II == trg
                        dogru = dogru+1;
                    end
                end
            end
        end
        dogru
        yanlis
        RD(q/5+2) = 100*dogru/(tgtltd*deneme)
    end
    toc
figure,
plot(q, RD ,'r*-')
grid on
```